Cutting a nerve of the hand alters the organisation of digit maps in primary somatosensory cortex

Martin Weber[1], Andrew Marshall[2], Ronan Timircan[1], Francis McGlone[3], Raffaele Tucciarelli[4], Obi Onyekwelu[5], Louise Booth[6], Edwin Jesudason[6], Vivien Lees[7,8], and Kenneth F. Valyear[1,9]

Author affiliations:

1. School of Psychology and Sport Science, Bangor University, Bangor, United Kingdom
2. Department of Musculoskeletal Biology, Institute of Life Course and Medical Sciences, University of Liverpool, Liverpool, United Kingdom
3. School of Life Sciences, Faculty of Science & Engineering, Manchester Metropolitan University, United Kingdom
4. School of Psychological Sciences, Birkbeck, University of London, London, United Kingdom
5. Department of Plastic Surgery, Portsmouth Hospitals University NHS Trust, Cosham, United Kingdom
6. Department of Orthopaedics and Trauma, Betsi Cadwaladr University Health Board, Bangor, United Kingdom
7. Department of Plastic Surgery, University of Manchester, Manchester, United Kingdom
8. Manchester University Foundation Hospitals Trust, Manchester, United Kingdom
9. Bangor Imaging Unit, Bangor University, Bangor, United Kingdom

Corresponding author:

Ken Valyear
School of Psychology and Sport Science
355 Brigantia Building,
Bangor University
Gwynedd, Wales, UK
LL57 2AS
k.valyear@bangor.ac.uk

Abstract

Hand nerve transection injuries precipitate a variety of reorganisational changes in both the peripheral and central nervous systems. Surgical repair restores the continuity of severed nerves, yet regenerating fibres establish new connections without topographical guidance, rearranging the branching architecture of peripheral nerves in the hand.

In non-human primates, forelimb nerve transection and repair dramatically alters the otherwise orderly and highly conserved organisation of the digit maps in primary somatosensory areas 3b and 1. Digit-map organisation becomes patchwork and highly variable. Although without compelling evidence, these same reorganisational changes are presumed to occur in humans and to have significant functional implications for patient recovery. In the current study, we evaluate these assumptions.

Functional MRI is used to characterise the fine-grained organisation of digit responses in the primary somatosensory cortex in twenty-one patients with nerve transection injuries and thirty healthy controls. Both univariate dice 'overlap' coefficients and state-of-the-art multivariate representational distances are used to quantify the extent and pattern of interdigit response separability in primary somatosensory cortex. Our results reveal significant differences between patients and controls. The fine-grained organisation of the primary somatosensory cortex is altered in nerve repair. Average dice coefficients reveal significantly increased interdigit response overlap. These effects are specific to the hemisphere contralateral to the nerve-repaired hand, reflecting inputs from reinnervated digits, and are more robust within the cortical zones of the repaired nerves. Nerve repair also alters the relative functional structure of the primary somatosensory cortex, changing the otherwise stereotypical pattern of interdigit response separability seen in healthy controls. Unexpectedly, these later alterations manifest bilaterally, as maps for the healthy hand of patients also show an atypical pattern of interdigit response separability.

Our findings provide the first compelling evidence for altered digit maps following nerve repair in humans, bridging results from animal models. Nonetheless, the clinical significance of the changes we observe remains unclear. No reliable relationships between fMRI measures of cortical reorganisation and behavioural measures of functional impairments are observed. Altered digit maps are not found to correlate with impairments in touch localisation or with broader measures of functional impairment as captured by sensory Rosen scores.

Introduction

Hand nerve injury constitutes a significant healthcare challenge. Incidence rates[1] and economic costs[2] are high, while patient recovery is typically incomplete[3,4]. Rehabilitation involves a complex interplay between peripheral and central factors[4,5]. Understanding how the brain changes and the clinical significance of those changes are major priorities.

When a nerve of the hand is cut and surgically repaired, nerve regeneration proceeds without topographical guidance[5-8]. Sprouting fibres innervate terminal receptors at different locations relative to the preinjury organisation, changing the structure of inputs from the hand to the central nervous system. In non-human primates, nerve transection and repair dramatically alters somatotopic organisation at multiple stations of the neuroaxis, including the fine-grained functional organisation of the digit maps in cortical areas 3b and 1[9-13]. Here, for the first time, we evaluate whether similar brain changes occur in humans.

Primate somatosensory area 3b comprises a finely organised map of the hand[14,15]. Those neurons encoding nearby regions are grouped together forming spatially segregated functional maps. The relative spatial arrangement of these cortical maps is highly consistent across individuals. In the lateromedial direction, the maps for each digit are arranged in sequence, with interdigit map boundaries delineated by cell-poor septa[16].

The functional maps of the hand are dramatically altered following nerve transection and repair in non-human primates[9-12]. Unlike the single continuous receptive fields observed normally, many cortical units now respond to multiple discontinuous locations on the hand, sometimes spanning multiple digits. Other cortical units exhibit normal single receptive fields, yet the typical spatial correspondence between the hand and cortex is altered. The digit maps are transformed from an orderly sequence that is highly conserved between individuals to a patchwork arrangement that is highly idiosyncratic. Touch of the same discrete patches of skin on the hand can also activate neurons that are non-adjacent within the cortical sheet, and some neurons exhibit large Pacinian-like receptive fields, not normally present in area 3b[14,15,17].

The cortical changes described above depend on nerve regeneration in the periphery. Different changes are observed after nerve transection and ligation[18,19], preventing nerve regeneration, as with amputation[20]. Purposeful crossing of peripheral nerves results in predictable changes in cortical topography[21]. Joining the proximal end of the ulnar nerve with the distal end of the median nerve, so that regenerating axons reinnervate the median-nerve-zone of the hand yet connect to the brain via the ulnar nerve, results in the emergence of cortical responses to touch of the median-nerve-zone of the hand within the ulnar-nerve-zone of cortex.

The current study examines whether nerve repair in humans alters the fine-grained organisation of the hand maps in primary somatosensory cortex (S1). The above evidence motivates two hypotheses. First, ***H_1 decreased separability***, digit responses in S1 should be more difficult to distinguish in patients recovering from nerve repairs. The overall separability of interdigit responses should decrease. Second, ***H_2 decreased typicality***, the relative spatial arrangement of the digit maps should change. Rather than the typical sequential ordering of D1-through-D5, nerve repair patients are expected to show an atypical patchwork arrangement, and the specific pattern of this arrangement is expected to show significant variation between individuals.

To evaluate these hypotheses, we use fMRI to quantify the pattern and extent of separability of interdigit responses in S1. While the precise position of individual digit response maps varies considerably between individuals, including the number and position of response 'peaks', the pattern of interdigit response separability is highly consistent[22,23]. Neighbouring digit responses are less separable, and the degree of separability between response maps generally declines as a function of their relative distance along the cortical sheet. In nerve repair, misdirected nerve regeneration is expected to alter this pattern (Fig. 1). Previous studies lacked the methods necessary to investigate functional changes at this level of detail.

We also sought to determine whether brain changes in nerve repair have functional consequences, focusing primarily on touch localisation (locognosia). Locognosia errors in nerve repair may be explained by reinnervation errors[24,25]. Given that these reinnervation errors may also explain changes in the functional organisation

of S1, as discussed above, it follows that changes in S1 may correlate with impaired locognosia.

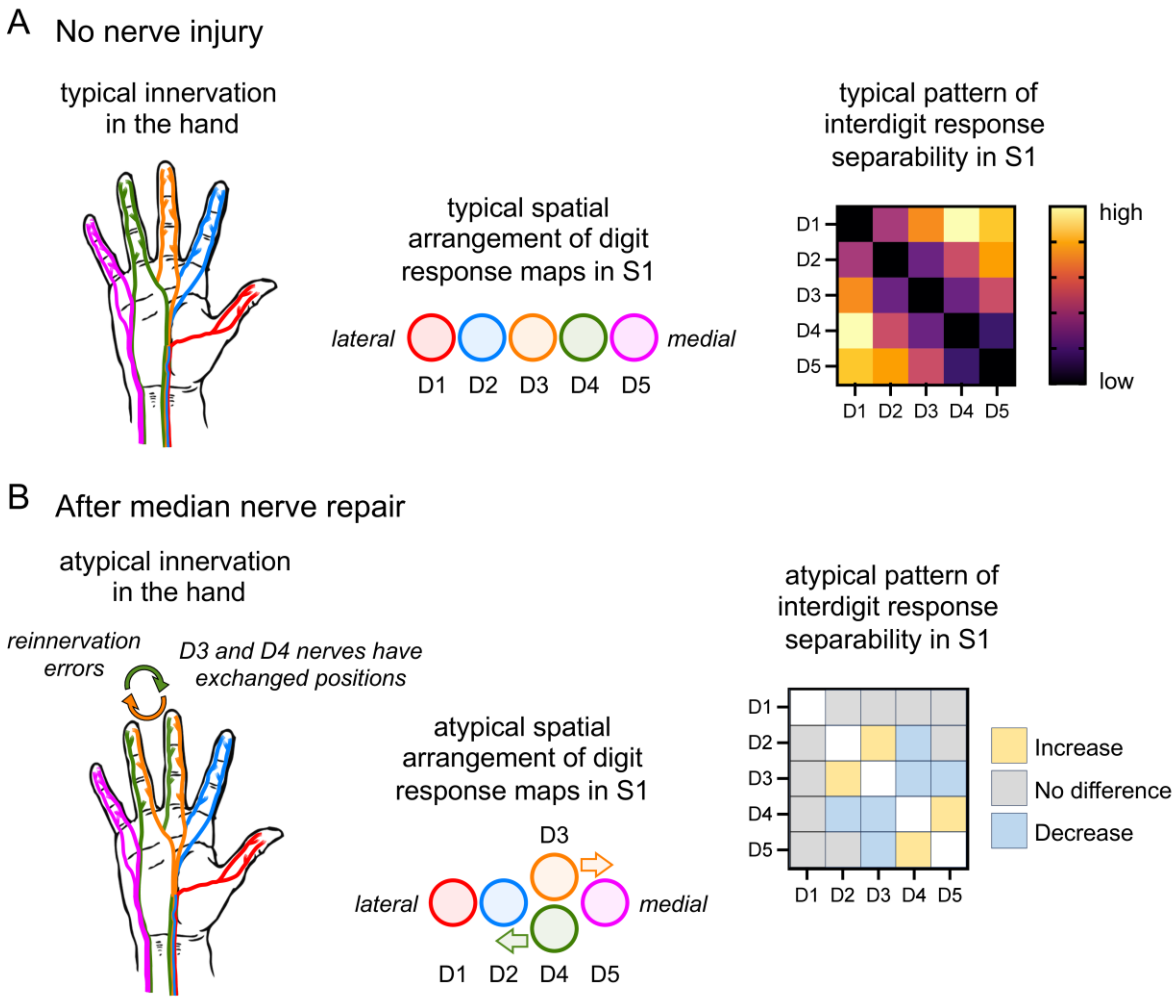

Figure 1. Reinnervation errors may alter the pattern of interdigit response separability in S1. A: The typical pattern of nerve innervation in the hand (left), the typical arrangement of digit maps in S1 (middle), and the typical pattern of interdigit response separability in S1 (right). The pattern of interdigit response separability is merely estimated based on prior results[22]. Neighbouring digit maps are less separable, thumb responses are more distinct, and the separability of D1-vs-D4 is greater than D1-vs-D5. **B:** After nerve transection and repair, regenerating fibres establish new connections without topographical guidance. Nerves may reroute to different digits or exchange between digits. Shown is a theoretical example where D3 and D4 nerves have exchanged positions after median nerve transection and repair (left). This would be expected to alter the relative spatial arrangement of digit response maps in S1 (middle) and the pattern of interdigit response separability (right). The pattern would deviate from the otherwise highly stereotypical and conserved pattern defined in healthy controls.

Materials and methods

Participants

Procedures were approved by the Bangor University local Ethics Board. All participants gave informed written consent according to the Declaration of Helsinki. Participants received financial compensation.

Patients

Twenty-one patients completed testing (age range: 19—75 years; mean age: 34.6 years; see Supplementary Table S1). Eighteen patients had complete transection injuries: ten ulnar, three median, and five ulnar and median ('both'). Three patients had incomplete transection injuries of the median nerve. One patient's injury was due to self-harm. This patient was deemed mentally stable when tested. All other injuries were of traumatic origin. All patients were injured in adulthood.

Healthy controls

Thirty participants completed testing (age range: 19—63 years; mean age: 31.9 years; 13 female). Two participants were left-handed.

MRI

A Philips 3T Ingenia Elition X MRI scanner with a 32-channel headcoil was used. Functional scans involved vibrotactile stimulation of the distal digit pads of the hand using custom-built stimulators (Supplementary Fig. S1). Each digit was stimulated seven times per scan, with each hand tested separately. Stimulation lasted 4s with bursts at 30Hz (500ms on, 500ms off). Scans began and ended with rest periods, involving fixation only, and included five additional rest periods (13-16s) interspersed throughout. Condition order was pseudo-randomised within scans, controlling for condition history, and sequence order was counterbalanced between participants. Total run duration was four minutes.

Stimulators were held using a custom-built base, which followed the hand's curvature and allowed adjustment to accommodate different hand sizes. The actuating terminus of each stimulator was aligned with the whirl of each digit. In cases where

patients had difficulties straightening their fingers, tape was used to fixate the stimulators.

Participants fixated a cross on a screen viewed through mirrors and paid attention to each stimulation. After each scan, they verified that stimulation was felt at each finger.

Stimulator amplitudes were standardised for all participants. Mechanical measurements were taken prior to the study to set the displacement amplitude of 'stronger' stimulators to approximate that of the 'weakest' stimulator.

All patients perceived stimulations to all digits, though some reported that the felt sensations were not localised to the distal end of the digit. No patient experienced pain during stimulations.

Scanning was completed in two sessions, one per hand, each comprising five functional scans and a field map scan. The first session included an anatomical scan. Each session took approximately 30 min.

The injured hand was always tested first to prioritise its measurement in case of early discontinuation, which occurred with one patient due to anxiety. This patient completed four scans with their injured hand and three scans with their uninjured hand. All other participants completed all scans. For healthy controls, hand order was counterbalanced.

Functional scans were taken at an in-plane resolution of 2 x 2 mm (T_2*-weighted echo-planar sequence, TR = 2s, 58 contiguous interleaved slices with 2 mm thickness, matrix size = 112x110, multiband = 2, bandwidth = 1905 Hz/pixel). The T_1-weighted structural scan was acquired using an MP-RAGE pulse (1mm isotropic, field of view = 225x225x175 mm). Field maps were acquired using a double gradient echo sequence. Field maps were not collected for the first six participants due to technical problems. These participants were healthy controls.

MRI analysis

MRI data were analysed using FSL (v6.0, http://www.fmrib.ox.ac.uk/fsl/)[26]. Non-brain structures were removed using BET. Head movement was processed using MCFLIRT. EPI unwarping was performed using FSL PRELUDE and FUGUE. High-pass filtering

(90s cut-off) was applied. Functional data were registered to structural scans using boundary-based registration[27].

The hemodynamic response function was modelled as independent predictors locked to the onsets and set to the durations of each vibrotactile stimulation event per condition: D1, D2, D3, D4 and D5. Additional covariates included the mean time series of the whole-brain and single-point predictors for high-motion outliers identified using FSL Motion Outliers.

First-level contrasts of parameter estimates were calculated for D1 > rest, D2 > rest, D3 > rest, D4 > rest, and D5 > rest. Second-level analyses were performed for each participant by combining first-level analyses (i.e., all functional runs per hand) using a fixed-effects model.

Regions of interest

Each participant's anatomy defined their S1 region of interest (ROI) per hemisphere, using the anatomical scan to identify the central sulcus. The maximal convexity of the central sulcus was taken as the likely location of the hand knob[28]. The central sulcus was traced manually at 10 mm above and below the hand knob. An attempt was made to restrict selection to the sulcus and avoid pre- and post-central gyri. Locations at the intersection of multiple sulci were included. Manual tracing was performed on a functional scan volume aligned to the anatomical, with enhanced image contrast. All tracings were completed by the lead author.

The ROI is named S1 rather than 3b, given inclusion of area 3a and likely some of area 1.

Measuring digit map separability

The separability of interdigit responses was measured using univariate dice ('overlap') coefficients[29] and multivariate representational distances[30]. Dice coefficients reflect the level of shared (minimally thresholded) positive-going activity between pairs of digit response maps. Greater values indicate more overlap. Representational distances reflect the level of dissimilarity between pairs of unthresholded digit response patterns. Greater values indicate greater separability.

Dice ('overlap') coefficients

Five contrasts were performed per hand per participant: D1 > rest, D2 > rest, D3 > rest, D4 > rest, D5 > rest. Resultant activity was thresholded at z = 2.0, uncorrected, selecting only positive-going responses[31,32]. Only active voxels within the anatomically defined contralateral S1 ROI were used to compute dice coefficients, quantifying the overlap between digit response maps. Dice coefficients were computed using the minimum-cluster normalised method, dividing the number of shared voxels by the number of voxels in the smaller map.

$$D_{AB} = \frac{A \cap B}{\min(A, B)} \qquad (1)$$

Formula 1. 'A' is the number of voxels comprising one digit response map and 'B' is the number of voxels comprising another digit response map. This produces measures of dice overlap ranging from 0 to 1. A dice coefficient of 0 indicates no overlapping activation between digit maps, and 1 indicates complete overlap.

If a smaller map sits entirely within a larger map, the dice coefficient is 1. This method has been used previously to quantify interdigit fMRI response separability in S1[32].

Representational distances

Representational distances were calculated for each pair of digit response maps as cross-validated squared Mahalanobis distances (using the toolbox from Nili *et al*[33] adapted for FSL[34]). For each digit response map, beta values from all voxels within the contralateral S1 ROI formed the complete pattern of responses. This includes all (unthresholded) beta values; the full-spectrum of positive- and negative-going fMRI responses. Extracted betas were then prewhitened using the voxel-wise residuals, and each run was used as an independent cross-validation fold to compute average (cross-validated) Mahalanobis distances across folds[30]. If two response patterns differ only in noise, their representational distance will be zero. Computing all pairwise interdigit distances generates a representational distance matrix with 10 unique measures.

Evaluating hypotheses

Dice coefficients and representational distances were computed for each participant and hemisphere ROI. Predictions regarding functional changes due to nerve repair are specific to S1 contralateral to the repaired hand, *S1-repaired*. To evaluate our hypotheses, we performed two tests for each measure (dice coefficients and representational distances; see Supplementary Methods for additional details). First, we compared *S1-repaired* against measures from healthy controls, *S1-controls*. Second, we compared *S1-repaired* against measures taken from the patient's healthy hand, *S1-healthy*. Additionally, we tested *S1-healthy* against *S1-controls* where no differences were predicted.

Data from healthy controls were extracted from the contralateral S1 ROI of each hemisphere and averaged. This approach was validated through additional analyses, confirming no impact of averaging between hands on comparisons against patients (Supplementary Results).

H_1 decreased separability

Nerve repair should decrease the separability of interdigit responses in S1. Larger dice coefficients and smaller representational distances are predicted.

Repair-zone-specific analyses

Previous findings from monkey neurophysiology indicate that cortical changes in areas 3b/1 are specific to digit response maps within the zone of the repaired nerve(s)[9-12]. We repeated tests of H_1 using only those dice-coefficients/representational-distances computed based on comparisons between maps within the nerve repair zone (Supplementary Methods).

H_2 decreased typicality

Nerve repair is expected to transform the typical arrangement of digit responses maps in S1. Patients should deviate from the stereotypical arrangement of interdigit separability observed in healthy controls.

Typicality scores were computed for each participant by comparing their interdigit separability patterns (both dice and representational distances) against the group mean pattern in healthy controls, generating an r-value for each measure. The

r-values reflect the degree of correspondence between an individual's pattern and the control group mean. High typicality indicates close agreement with the normative pattern, while low typicality indicates divergence.

To estimate typicality in controls, we used a leave-one-subject-out analysis, comparing each individual's pattern against the mean pattern of all other controls.

Behavioural tests

Locognosia

Locognosia was measured using the Digital Photograph Method, detailed previously[35]. Nineteen of 21 patients completed testing (Supplementary Table S1).

Briefly, the participant's hand was blocked from their view and points were marked on the volar surface using an ultraviolet (UV) pen (Supplementary Fig. S2). These points served as targets for touch stimulation. Two photographs were taken, one with and one without UV lighting, rendering targets seen and unseen, respectively. The experimenter used the photograph with visible targets to register their locations, and participants reported the felt position of each stimulation on the photograph with unseen targets.

We report two measures: (1) absolute error, the Euclidian distance between target-response pairs in millimetres; and (2) Misreferrals, responses made to an incorrect digit or to the palm of the hand. Misreferrals are excluded from the calculation of absolute error.

Sensory Rosen scores

The Rosen test is a standardised assessment of hand function after median/ulnar nerve repair[3,36]. All 21 patients completed the sensory and pain domains; the motor domain was not tested. Procedures followed standard protocols[37]. Touch detection thresholds used Semmes-Weinstein monofilaments; two-point discrimination used The Two-Point Discriminator (Exacta Precision & Performance, 2019 North Coast Medical, Inc.). Shape-texture-identification and the Sollerman test materials were produced in-house.

Results

Validating controls data

To evaluate our hypotheses regarding functional brain changes in patients, we quantify interdigit response separability in S1 using dice coefficients and representational distances. Critically, the normative pattern is known from previous research[22] (Fig. 1A). Responses from topographically adjacent digit-maps, '1st neighbours', are less separable than those of 2nd, 3rd, and 4th neighbours, and separability generally increases with increasing neighbourhood position. One exception is that thumb responses tend to separate from ring-finger responses more than from little-finger responses. Thumb responses are also more distinct. These detailed characteristics define the normative pattern of interdigit response separability in S1. They provide objective means to evaluate the quality of our data from healthy controls and validate its use as a benchmark for comparison against patients.

Our results replicate previous findings. Both dice coefficients (Fig. 2A/B) and representational distances (Fig. 2C/D) reveal a systematic gradient of increasing interdigit response separability with increasing neighbourhood position. A significant main effect of neighbourhood position is confirmed (dice: $F(3, 87) = 90.0$, $p < 0.0001$; representational distances: $F(3, 87) = 106.1$, $p < 0.0001$). Post-hoc comparisons reveal a stepwise increase in separability with increasing neighbourhood position (dice: 1st > 2nd > 3rd > 4th, all t-values > 3.3, p-values < 0.005; representational distances: 1st > 2nd > 3rd > 4th, all t-values > 3.6, p-values < 0.005). The results validate our controls data for comparison against patients.

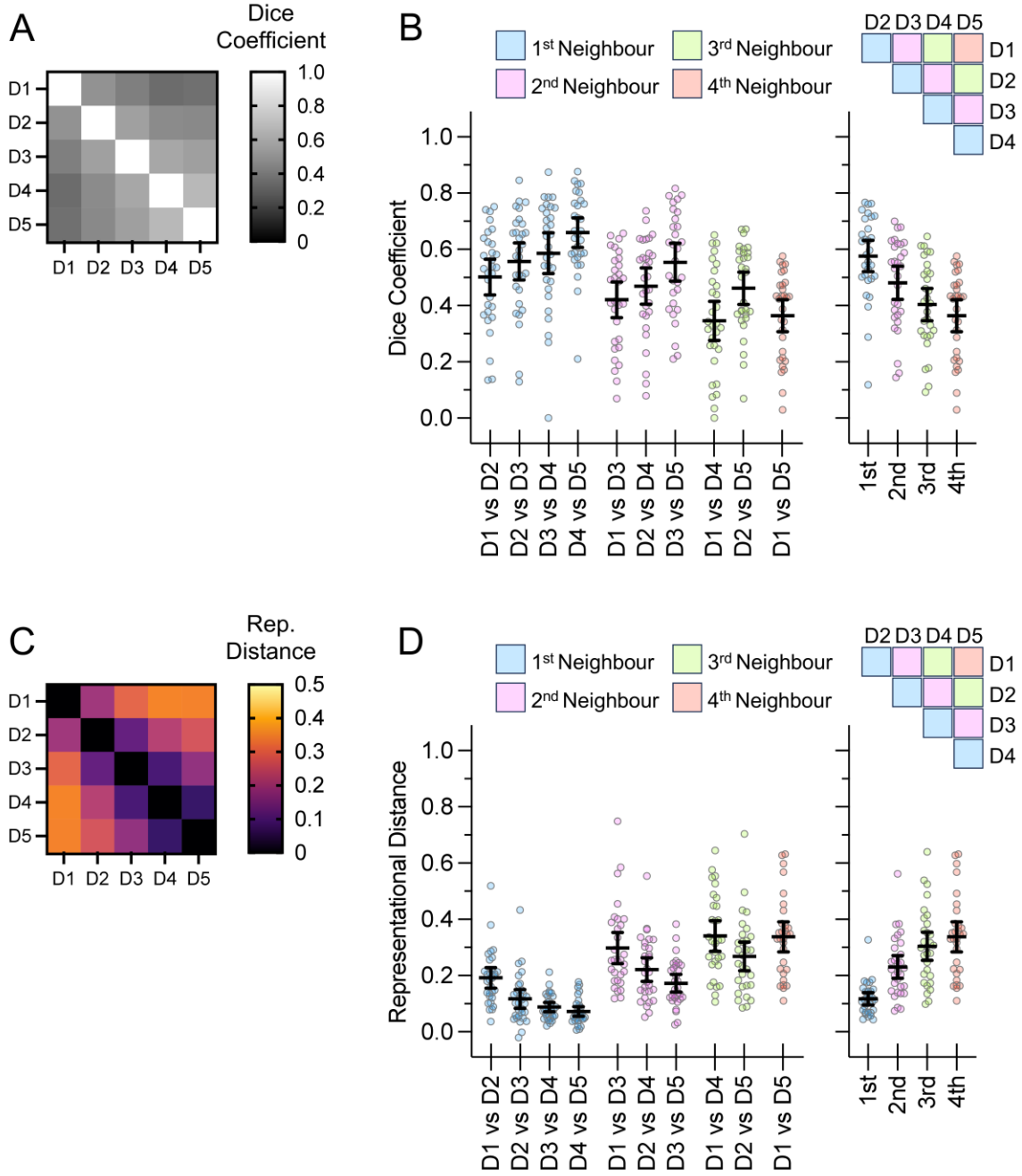

Figure 2. Interdigit response separability in healthy controls. A: Univariate dice ('overlap') coefficients reflect the degree of overlap between interdigit responses. The 'heatmap' shows the group mean dice coefficients across all possible (10) pairwise digit comparisons. Lighter shading indicates larger dice coefficients; greater response overlap. **B:** Same data as in A, yet with individual-level results. Error bars are 95% confidence intervals around the group means. The results of each comparison are color-coded according to neighbourhood position. The right-most plot shows the aggregate data. Note the stepwise decrease in overlap with increasing neighbourhood position. **C:** Multivariate representational distances reflect the degree of dissimilarity between pairs of unthresholded digit responses. Greater values indicate more distinct activation patterns. The 'heatmap' shows the group mean representational distances across all possible (10) pairwise digit comparisons. **D:** Same data as in C, yet with individual-level results. Error bars are 95% confidence intervals around the group means. The plots are otherwise organised as in B, yet for representational distances. Note the stepwise increase in representational distances with increasing neighbourhood position.

Evaluating *H_1 decreased separability*

Dice coefficients

Fig. 3A and 3B provide the group mean dice coefficients of patients and healthy controls. The organisation is the same as in Fig. 2A and 2B; data from controls are repeated here for ease of comparison.

Average dice coefficients reveal significantly increased interdigit response overlap in patients with nerve repairs, consistent with ***H_1 decreased separability*** (Fig. 3C-i). Digit response maps overlap to a greater extent in *S1-repaired* compared to *S1-healthy* ($t(20) = 2.7$, $p = 0.01$) and *S1-controls* ($t(49) = 2.2$, $p = 0.03$), and no differences are observed between *S1-healthy* and *S1-controls* (Mann-Whitney $U = 288$, $p = 0.61$). Nerve repair increases the degree of overlap between digit responses in S1, and these effects are specific to the repaired hand.

Since monkey electrophysiological data indicate that changes in S1 are restricted to cortical zones of the repaired nerves[9-12], we repeat these analyses using only those estimates of interdigit response overlap corresponding to maps within the nerve repair zones (see 'Materials and methods'). The results again reveal increased interdigit response overlap in nerve repair specific to *S1-repaired* (Fig 3C-ii). Dice coefficients are greater in *S1-repaired* than both *S1-healthy* ($t(20) = 2.8$, $p = 0.01$) and *S1-controls* ($t(49) = 2.8$, $p = 0.008$), and no differences are observed between *S1-healthy* and *S1-controls* ($t(49) = 0.1$, $p = 0.92$).

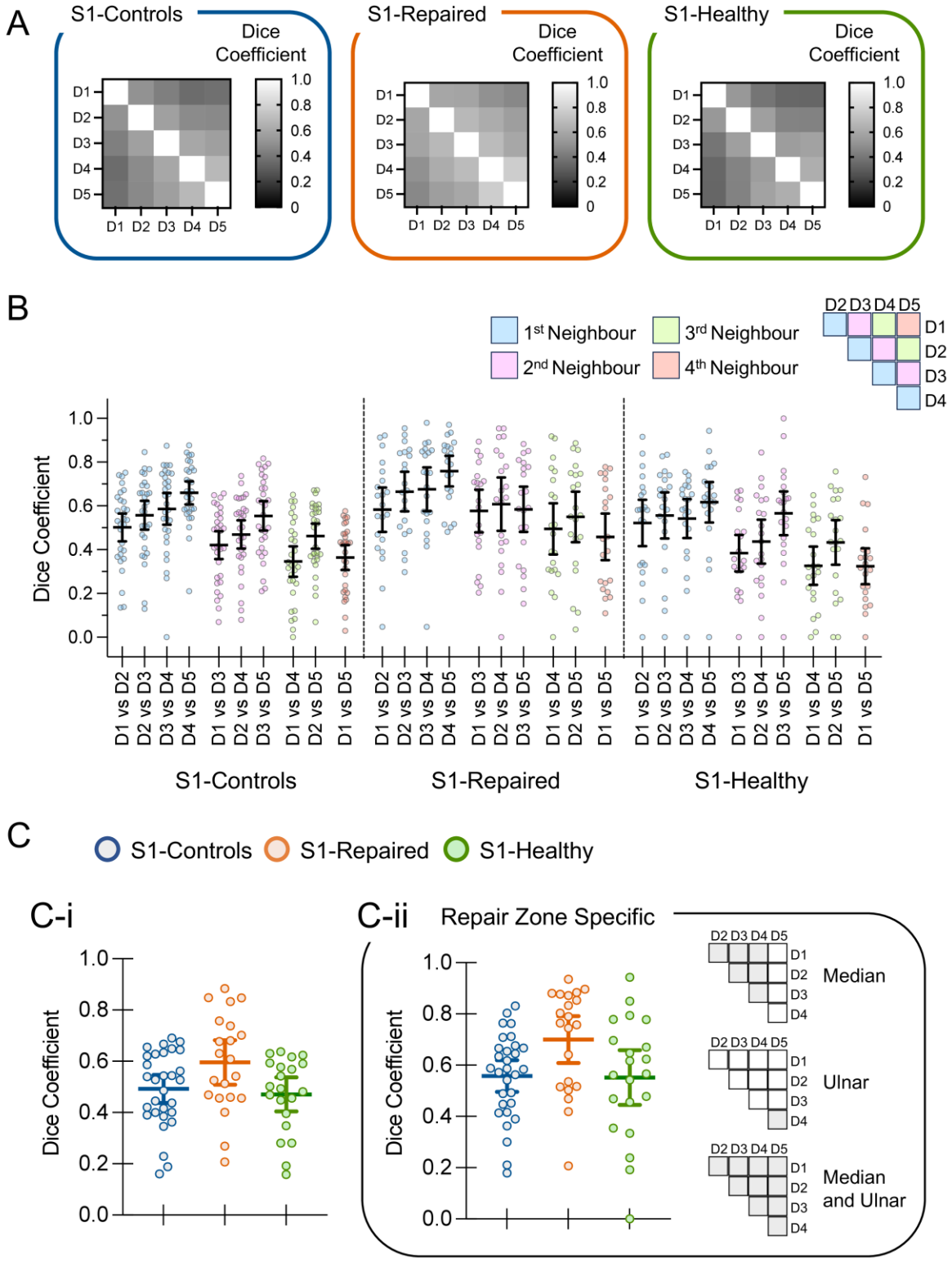

Figure 3. Evaluating H_1: Dice. A: Group mean dice coefficients are shown as heatmaps for *S1-controls*, *S1-repaired*, and *S1-healthy*. **B:** Same data as in A, yet with individual-level results. Error bars are 95% confidence intervals around the group means. Data are color-coded according to neighbourhood position. **C-i:** Group dice results across all interdigit comparisons. **C-ii:** Group dice results restricted to comparisons within the cortical zones of the injured nerves. The icons illustrate how these zones differ between patient subgroups.

Representational distances

Representational distances are shown in Fig. 4. Unlike dice coefficients, average representational distances do not reveal differences between patients and healthy controls (Fig. 4C-i). No differences are observed between *S1-repaired* and *S1-controls* (Mann-Whitney U = 274, p = 0.44), nor between *S1-repaired* and *S1-healthy* (Wilcoxon W = 13, p = 0.84). In other words, according to multivariate representational distances, nerve repair does not decrease the separability of interdigit responses in S1. As expected, no differences are observed between *S1-healthy* and *S1-controls* (Mann-Whitney U = 289, p = 0.63).

As with dice coefficients, we also restrict these analyses to the cortical zones of the repair nerves (Fig. 4C-ii). Statistically, the repair-zone-specific and unrestricted analyses yield the same results. Again, we find no reliable differences between *S1-repaired* and *S1-healthy* (Wilcoxon W = -17, p = 0.79), nor between *S1-repaired* and *S1-controls* (t(49) = 1.9, p = 0.07). No differences are observed between *S1-healthy* and *S1-controls* (Mann-Whitney U = 269, p = 0.39).

The results are inconsistent with those of the dice analyses. Representational distances, considering the full spectrum of fMRI responses, reveal no evidence for decreased interdigit response separability in nerve repair, inconsistent with ***H_1 decreased separability***. Conversely, dice coefficients, based on thresholded positive-going fMRI responses, reveal diminished interdigit response separability in nerve repair, and these effects are more robust within the nerve-repair-zone of S1.

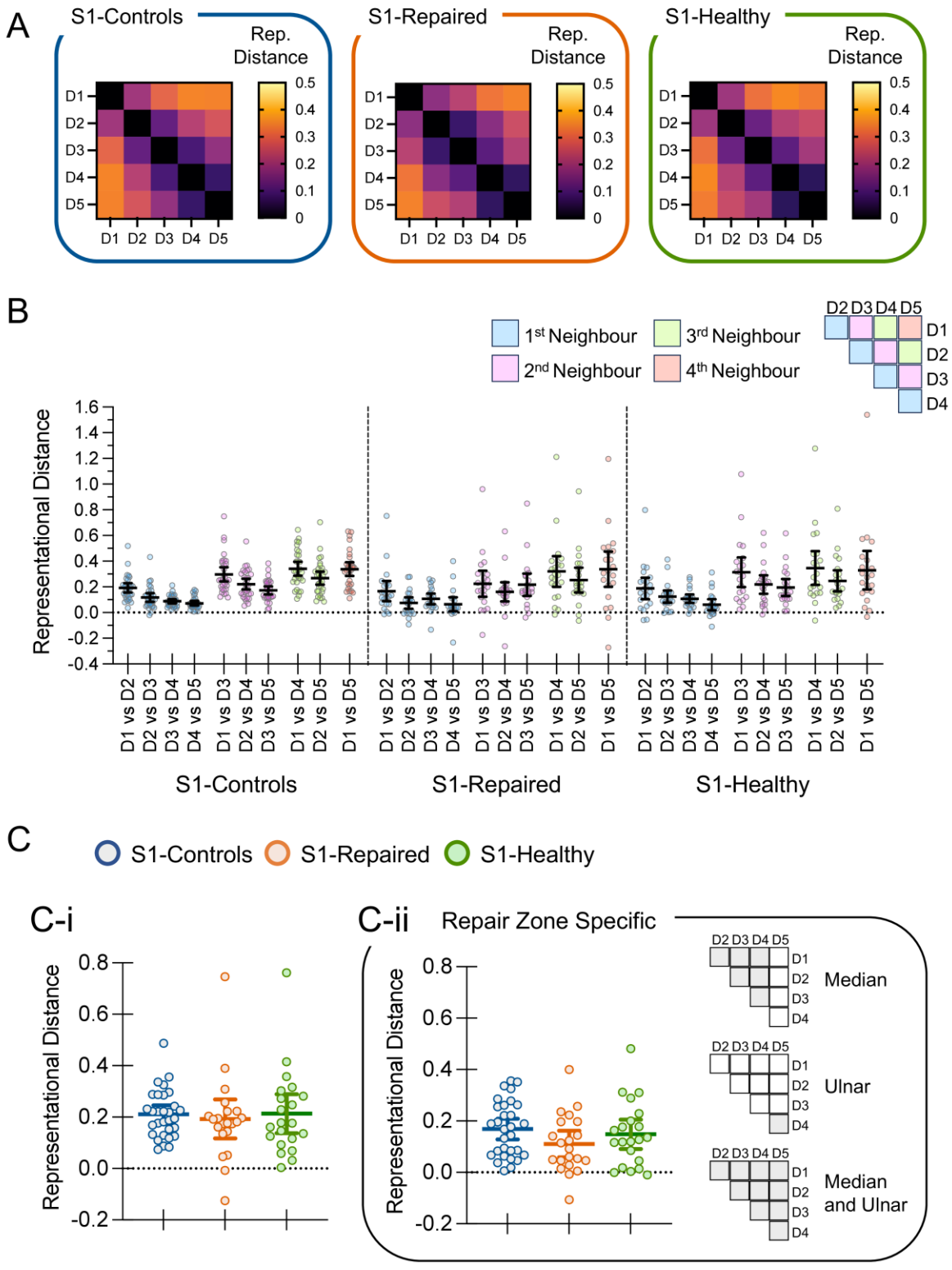

Figure 4. Evaluating H_1: Representational distances. A: Group mean representational distances are shown as heatmaps for *S1-controls*, *S1-repaired*, and *S1-healthy*. **B:** Same data as in A, yet with individual-level results. Error bars are 95% confidence intervals around the group means. **C-i:** Group dice results across all interdigit comparisons. Data are color-coded according to neighbourhood position. **C-ii:** Group representational distances results restricted to comparisons within the cortical zones of the injured nerves. The icons illustrate how these zones differ between patient subgroups.

Evaluating *H_2 decreased typicality*

Healthy controls exhibit a normative pattern of interdigit response separability (Fig. 2). This pattern is hypothesised to change after nerve repair.

Typicality provides a measure of agreement between an individual's interdigit response pattern and the normative pattern defined by healthy controls. High positive typicality indicates close agreement.

Dice coefficients

Fig. 5A provides examples of individual-level dice typicality per patient subgroup: median, ulnar, and 'both'. Typicality is shown with corresponding heatmaps. Group mean data from healthy controls are provided for reference.

Some patients closely resemble the normative pattern; for example, patient ID22, with an isolated ulnar nerve repair, has a typicality measure of r = 95. Inspection of this patient's heatmap shows close alignment with that of healthy controls. For example, the lightest cells of the matrix (highest dice values) fall along the off-diagonal, '1st neighbours', and the cell representing the comparison between D4-D5 shows the lightest shading. Conversely, other patients have a different pattern. ID34 has a typicality near zero, for example, and ID33 shows a pattern that is negatively correlated with that of healthy controls.

Quantitative group comparisons support ***H_2 decreased typicality*** (Fig. 5B). Nerve repair significantly alters the otherwise stereotypical pattern of interdigit responses observed in healthy controls. Dice typicality is decreased in *S1-repaired* compared to *S1-controls* (Mann-Whitney U = 162, p = 0.003). Unexpectedly, *S1-healthy* also shows decreased typicality compared to *S1-controls* (Mann-Whitney U = 194, p = 0.02), and *S1-repaired* does not differ from *S1-healthy* ($t(20) = 0.47$, p = 0.65). In other words, altered S1 maps are observed bilaterally.

Isolated ulnar nerve repairs might result in subtler changes, as primate models indicate restricted S1 remodelling, specific to the nerve-repair zone. To investigate this, we performed a patient subgroup analysis separating ulnar nerve repairs from median and 'both' repairs.

Fig. 5C shows these results. In *S1-repaired*, dice typicality is lowest for median or 'both' compared to ulnar repairs, consistent with less pronounced changes in

typicality in ulnar nerve injury. Crucially, however, these differences do not reach statistical significance. A mixed ANOVA reveals no significant interaction ($F(1,19) = 1.8$, $p = 0.19$), nor main effects of hemisphere ($F(1,19) = 0.17$, $p = 0.69$) or subgroup ($F(1,19) = 2.3$, $p = 0.15$).

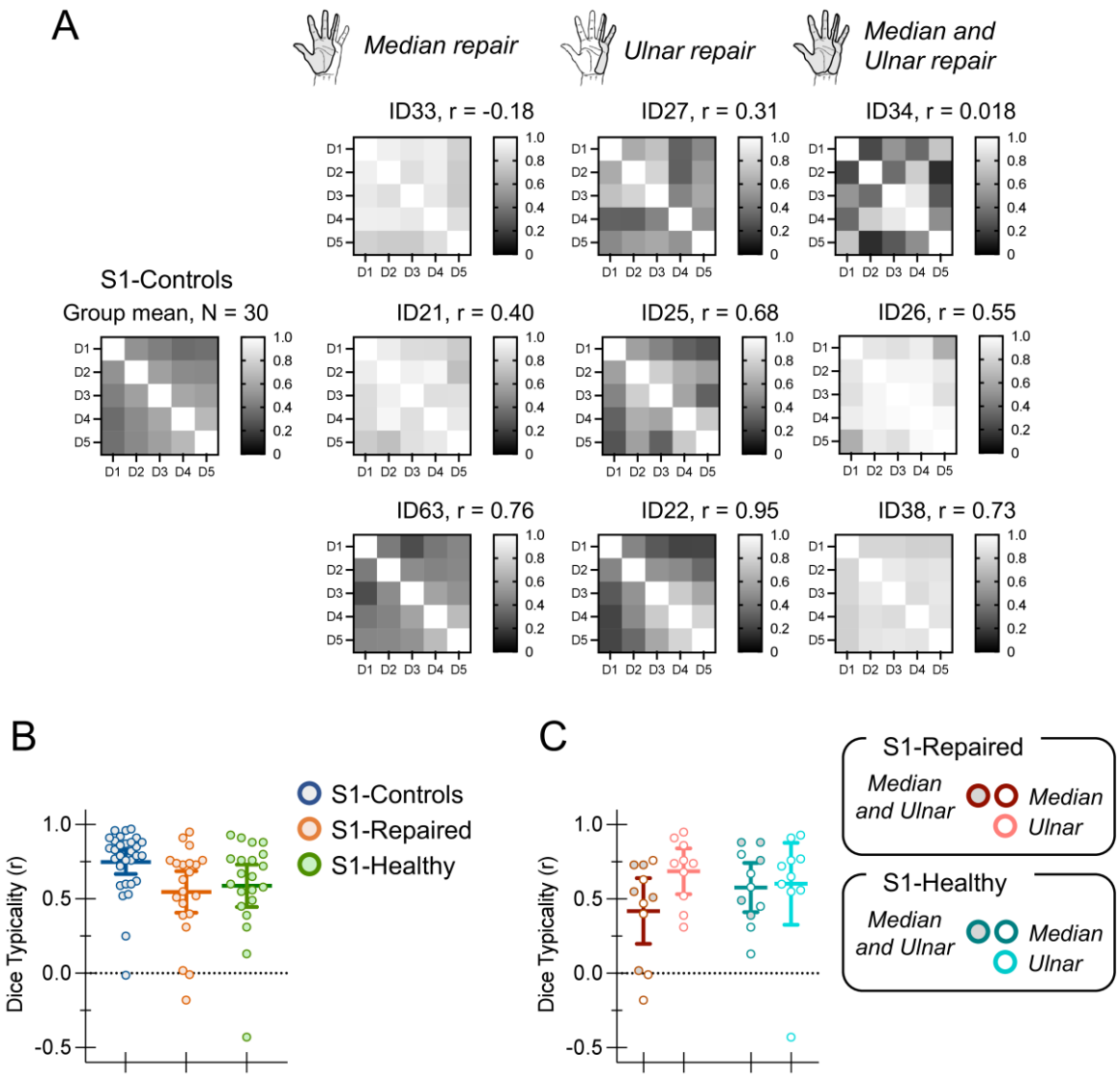

Figure 5. Evaluating H_2: Dice. A: Dice typicality from individual patients are shown, from *S1-repaired*. The patient with the lowest, intermediate, and highest typicality values are shown for each type of nerve repair: median, ulnar, and 'both'. Typicality is indicated with corresponding heatmaps. The group mean pattern in healthy controls is provided for reference. **B:** Group dice typicality is shown for *S1-controls*, *S1-repaired*, and *S1-healthy*. **C:** Dice typicality is shown for patient subgroup and hemisphere. Error bars in B and C are 95% confidence intervals.

Representational distances

Like dice typicality, representational distances typicality reveals considerable variability between patients (Fig. 6A). Some patients closely resemble the normative pattern, exhibiting high positive typicality scores, while others do not. ID46, a patient with an isolated median nerve repair, and ID34, a patient with repairs to 'both' nerves, show markedly atypical patterns. Qualitative inspection of their respective heatmaps against the normative pattern from controls shows clear differences. The patient patterns are atypical.

Group results are consistent with ***H_2 decreased typicality*** (Fig. 6B). Nerve repair alters the pattern of interdigit responses in S1. Typicality is decreased in *S1-repaired* compared to *S1-controls* (Mann-Whitney U = 155, p = 0.002). As with dice typicality, the observed effects are not restricted to *S1-repaired*. Typicality is also decreased in *S1-healthy* compared to *S1-controls* (Mann-Whitney U = 185, p = 0.02), and does not differ between *S1-repaired* and *S1-healthy* (t(20) = 1.73, p = 0.099).

As above, we reasoned that those patients with ulnar nerve injuries may show a pattern of interdigit responses that is relatively closer to that of healthy controls (i.e., less perturbed). If so, they should separate from patients who have had repairs to the median nerve, or repairs to both the median and ulnar nerves. Patients with median or 'both' nerve repairs should have lower measures of typicality.

Our results support this conjecture. In *S1-repaired*, typicality depends on patient subgroup (Fig. 6C). Patients with repairs to the median or 'both' nerves have significantly lower typicality compared to patients with isolated ulnar nerve repairs. These effects are specific to *S1-repaired*. In *S1-healthy*, typicality does not depend on patient subgroup. A mixed ANOVA reveals a significant interaction ($F(1,19) = 7.7$, $p = 0.01$), and no significant main effects (hemisphere: $F(1,19) = 3.5$, $p = 0.08$; subgroup: $F(1,19) = 4.0$, $p = 0.06$). Post-hoc comparisons confirm patient subgroup differences in *S1-repaired* ($t(19) = 2.67$, $p = 0.01$) but not in *S1-healthy* (Mann-Whitney U = 45, $p = 0.50$).

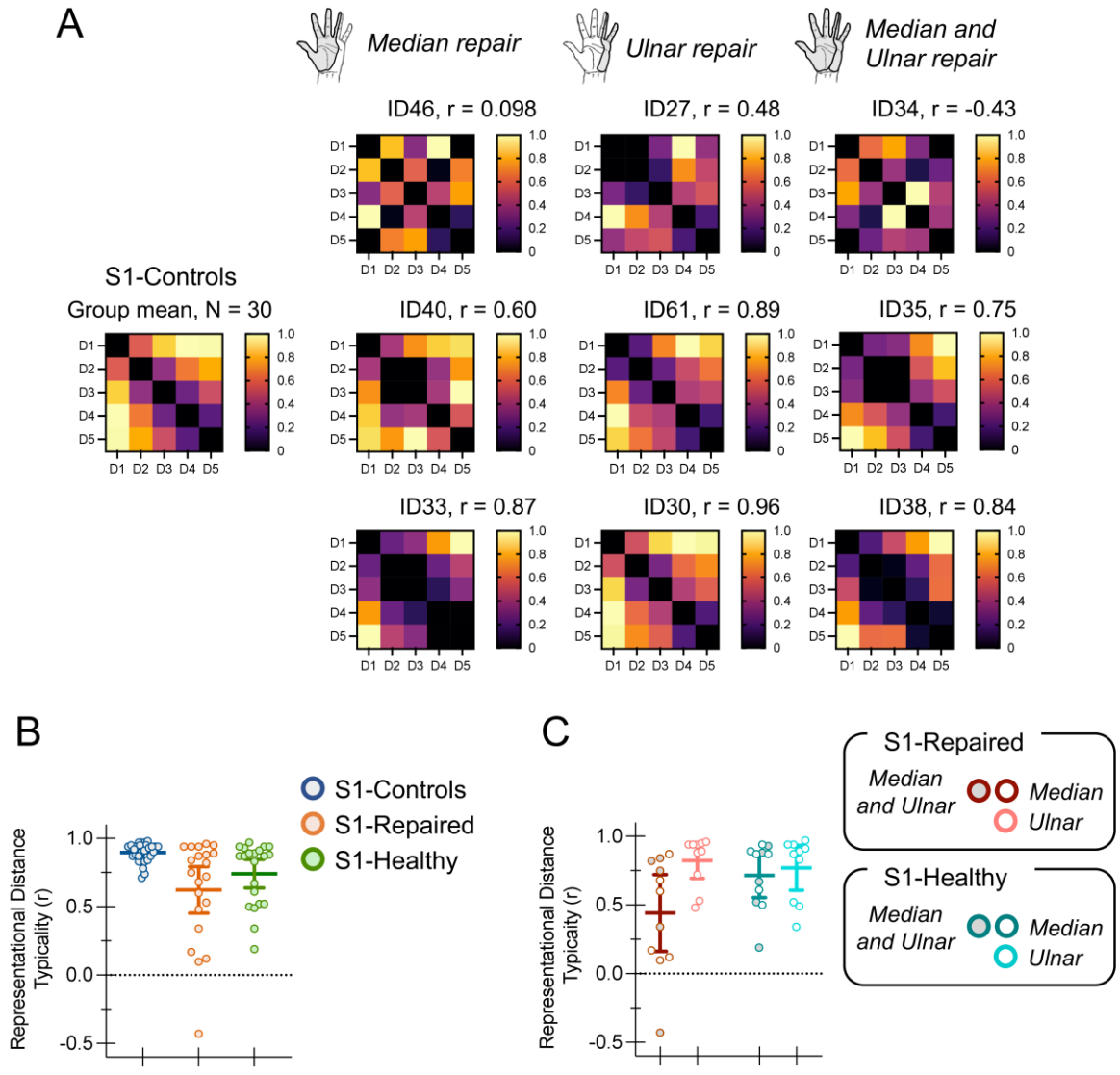

Figure 6. Evaluating H_2: Representational distances. A: Representational distances typicality from individual patients are shown, from *S1-repaired*. The patient with the lowest, intermediate, and highest typicality values are shown for each type of nerve repair: median, ulnar, and 'both'. Typicality is indicated with corresponding heatmaps. The group mean pattern in healthy controls is provided for reference. Representational distances are range-normalised to facilitate comparisons. **B:** Group representational distances typicality is shown for *S1-controls*, *S1-repaired*, and *S1-healthy*. **C:** Representational distances typicality is shown for patient subgroup and hemisphere. Error bars in B and C are 95% confidence intervals.

As reported above, although not statistically significant the same pattern of differences is evident for dice typicality (Fig. 5C). Together, the results are nonetheless reinforcing. Nerve repair decreases the typicality of interdigit response separability in S1 relative to healthy controls, and these differences are more pronounced when the median nerve, or both the median and ulnar nerves are involved. Patients with isolated

ulnar nerve repairs show less pronounced changes. This makes sense given that the ulnar nerve innervates fewer digits, and thus, less S1 territory has the potential to rearrange.

Do changes in S1 relate to functional impairments?

Our fMRI results reveal significant alterations in the functional organisation of S1 after nerve repair. Do these alterations have functional consequences? To investigate this, we conducted correlational tests between fMRI measures of functional change and the outcomes of two behavioural tests: (1) locognosia and (2) sensory Rosen.

Three fMRI results indicate functional brain changes: (1) increased dice coefficients (repair-zone-specific data); (2) decreased dice typicality; and (3) decreased representational distances typicality. These measures were compared against behavioural measures.

Locognosia

Nineteen patients completed locognosia testing using the Digital Photograph Method, with detailed results from eighteen patients (and thirty-three controls) reported previously[35]. Here, we evaluate whether locognosia performance in nerve repair correlates with functional brain changes.

Absolute error

Absolute error measures the difference between stimulated and perceived locations of touch, excluding misreferrals—errors made between digits, or from a digit to the palm (see 'Materials and methods'). Lower absolute error indicates better performance. A single patient's data is shown in Fig. 7A, for illustration.

Correlational tests reveal no evidence for a relationship between absolute error and average dice coefficients ($r(17) = -0.32$, $p = 0.18$), dice typicality ($r(17) = 0.05$, $p = 0.83$), or representational distances typicality ($r(17) = -0.38$, $p = 0.11$) (Fig. 7B). Patients who make larger errors in localising punctate, suprathreshold touch stimulation on their repaired hand do not necessarily show the largest differences in functional markers of nerve-repair-related changes in S1. No consistent relationships are observed.

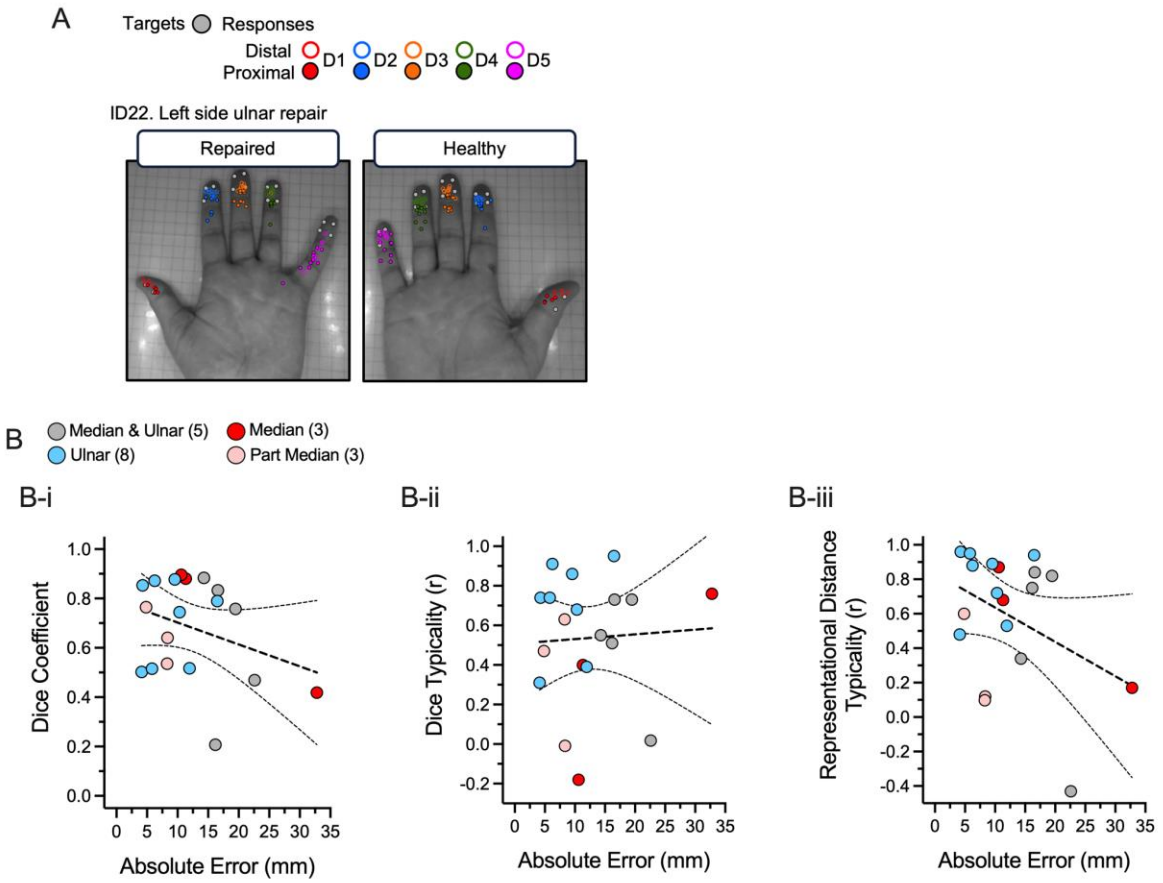

Figure 7. Absolute error of locognosia does not relate to S1 reorganisation. A: Locognosia results from a single patient with an isolated ulnar nerve injury. Targets (grey circles) and responses (coloured circles) are overlaid on the photographs of the hand. The colours indicate which digit were touched (see inset key). The patient shows a relatively large spread of responses (high absolute error) specific to D5 of their repaired hand. This figure has been modified from Weber et al.[35], licensed under CC-BY. **B:** Group-level (n = 19) correlational tests of absolute error versus dice coefficients (B-i), dice typicality (B-ii), and representational distances typicality (B-iii). No reliable relationships are observed.

Misreferrals

Misreferrals are generally infrequently observed; only three patients show abnormally high numbers of misreferrals, outside the range of healthy controls[35]. This makes quantitative comparisons against fMRI measures challenging (see Supplementary Results; Supplementary Fig. S3). However, descriptive results from two patients with unusual frequencies and patterns of misreferrals are nonetheless useful to visualise the potential links between misreferrals, reinnervation errors, and altered digit maps. We offer these results for conceptual purposes.

Patient ID21 consistently reports touch of the index finger as being felt on the middle finger, and sometimes vice versa (Fig. 8A). In other words, the index and middle fingers are often confused; a pattern not observed in healthy controls[35]. In principle, this could result from an exchange between digital nerves (Fig. 8B). Such reinnervation errors would predict specific alterations in the arrangement of the digit maps in S1, and thus the pattern of interdigit response separability. Fig. 8C compares the patient's pattern of representational distances against the normative pattern in controls. Some differences align with predictions (e.g., decreased D2-D3 separability), while others do not (e.g., increased D1-D5 separability). Patient ID32 also exhibits a pattern of misreferrals that could reflect reinnervation errors between digits (Supplementary Fig. S4).

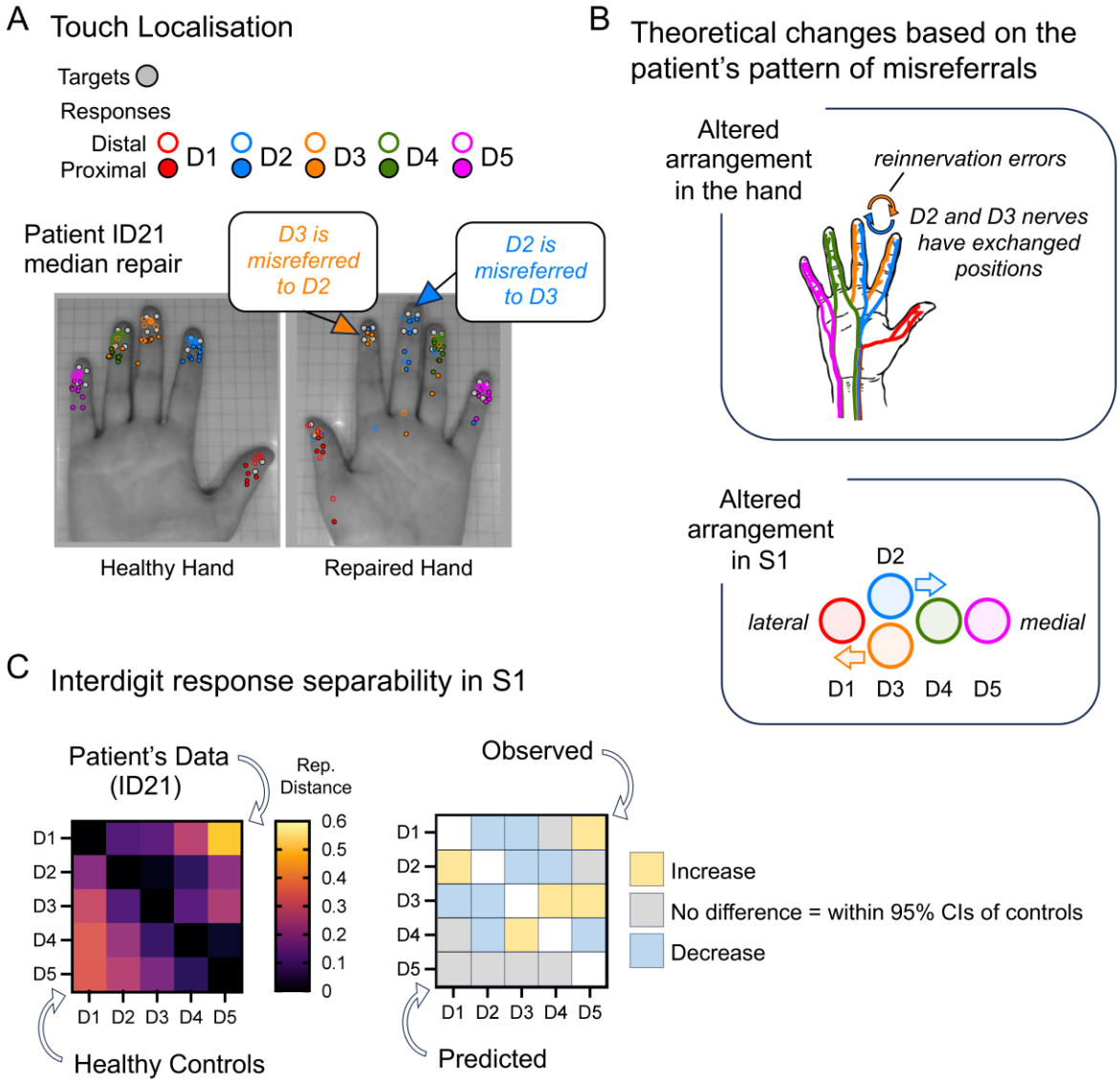

Figure 8. Frequent misreferrals between digits may reflect reinnervation errors. A: Locognosia results from patient ID21. Targets (grey circles) and responses (coloured circles) are overlaid on the photographs of the hand. The colours indicate which digits were touched (see inset key). Touch of D2 was frequently misreferred to D3, and sometimes vice versa. This figure has been modified from Weber et al.[35], licensed under CC-BY. **B:** Theoretical changes in the arrangement of nerves in the hand based on the patient's pattern of misreferrals. Reinnervation errors may have resulted in an exchange between D2 and D3 nerves. This would predictably alter the arrangement of digit maps in S1. For example, D2 should 'move closer' to D4. **C:** Representational distances are shown in the heatmap, with patient ID21's data above the reference diagonal and the mean of healthy controls below (left). Predicted and observed differences between the patient's data and controls (right). The observed differences are above the reference diagonal and predicted differences are below. For each interdigit comparison, 'increased'/'decreased' observed results indicates that the patient's representational distances are above/below the 95% confidence intervals of healthy controls, respectively.

Sensory Rosen scores

We also examine whether changes in S1 relate to sensory Rosen scores. The sensory Rosen test measures both low- and high-level sensory and motor hand function[36]. The best score possible is 1.0, indicating no impairment.

Our results reveal no evidence for a relationship between sensory Rosen scores and functional changes in S1 (Supplementary Fig. S5). Test performance does not correlate with average dice coefficients ($r(19) = 0.02$, $p = 0.92$), dice typicality ($r(19) = 0.06$, $p = 0.78$), nor representational distances typicality ($r(19) = -0.03$, $p = 0.90$).

Discussion

Surgical repair of the major nerves of the hand significantly alters the functional organisation of S1. Digit response maps overlap to a greater extent in patients with nerve repairs. This increased spatial response overlap is specific to the hemisphere contralateral to the site of nerve repairs and is greatest within the cortical zones of the repaired nerves, reflecting inputs from reinnervated digits. Nerve repair also alters the relative functional structure of S1, changing the otherwise stereotypical pattern of interdigit response separability seen in healthy controls. Unexpectedly, these later alterations manifest bilaterally, as maps for the healthy hand also show an atypical pattern of interdigit response separability.

Until now, altered maps of the hand have only been described in animal studies of nerve repair. For the first time, we have characterised the fine-grained organisation of S1 in patients with hand-nerve repairs and found that the typical orderly arrangement of the digit maps is significantly transformed. Our results provide a hitherto missing bridge between animal and human models of nerve repair. Nonetheless, the clinical significance of the changes we observe remains unclear. We do not find any reliable relationships between fMRI measures of reorganisation in S1 and behavioural measures of functional impairments. Our principal findings and their implications are discussed in detail below.

Increased overlap

Average dice coefficients reveal significantly increased interdigit response overlap in patients with nerve repairs. Different digits tend to activate the same parts of S1, indicating decreased spatial response specificity. These effects are specific to the hemisphere contralateral to the site of nerve repairs, and are statistically more robust within the cortical zones of the repaired nerves.

The findings are consistent with observations from animal models. Nerve repair in non-human primates precipitates various changes in the response properties of neurons in areas 3b and 1[9-12]. After nerve regeneration has taken place in the periphery, many cortical neurons respond to touch stimulation at multiple discontinuous locations on the hand. These ‘multi-field’ neurons are found within the cortical zone of the repaired nerve and can have up to five different response fields on

the hand, some of which may span multiple digits. This kind of change could explain our results. Stimulation of different digits may activate the same parts of S1, increasing measures of interdigit response overlap (i.e., dice coefficients). Animal models also reveal the emergence of cortical neurons with large Pacinian-corpuscle-like receptive fields, not normally present in area 3b, and neurons that are distant in cortical space yet respond to touch of the same discrete regions of skin on the hand. Such changes may also increase the likelihood of observing spatially overlapping cortical responses for the stimulation of different digits, consistent with our results.

Peripheral changes may explain these effects. Unusual ramification of branching nerve fibres follows nerve repair[5,6,38], and could explain the emergence of 'multi-field' neurons in S1. Afferent inputs normally conveying information from spatially continuous regions of skin now communicate signals from spatially disparate regions[25]. Reinnervation errors may also involve connections with end organs that differ in receptor-class from those of the pre-injury condition[39,40]. Such changes may explain the emergence of 3b neurons with larger-than-typical receptive fields[10]. Altered axonal-receptor pairings may contribute to the unusual or painful sensations commonly experienced in nerve repair, reported by most (90%) of our patient group (Supplementary Table 1).

The effects of increased interdigit response overlap are specific to dice coefficients. Representational distances show no reliable differences between patients and controls. This discrepancy indicates that although positive (minimally) thresholded fMRI responses show greater overlap in nerve repair, the full spectrum of activity across all voxels within S1, including both positive- and negative-going responses, remains distinct.

This discrepancy might indicate closer agreement between neural information measured using classic electrophysiological 'mapping' techniques and neural information measured using conventional fMRI contrast methods, as opposed to multivariate analysis methods. In the animal studies of nerve repair, functional maps are defined by neural spiking. Patterns of response inhibition are not considered, nor are the response preferences of other cells. This approach to functional mapping may give results that more closely agree with measures of the spatial extent of overlap between positive thresholded fMRI responses—i.e., dice coefficients—than with measures of the similarity between unthresholded patterns of fMRI responses—i.e.,

representational distances. While positive fMRI responses reflect both increased spiking and changes in postsynaptic potentials[41], which may include inhibitory signals, unthresholded multivoxel patterns of fMRI responses include negative-going signal-changes likely to reflect response inhibition.

Atypical organisation

Nerve repair alters the pattern of interdigit response separability in S1. In healthy controls, this pattern reflects the spatial topography of digit maps and the probabilistic patterns of finger movements made in everyday life[22]. Our results reveal a significant departure from this pattern in nerve repair.

The data agree with observations from animal models. Following forelimb nerve transection and repair in non-human primates, the typical orderly arrangement of digit maps is transformed in S1[9-12]. The normative pattern of skin-to-cortex adjacencies is altered. The pattern becomes patchwork and highly variable between individuals.

Peripheral reinnervation errors may drive these effects. Since nerve regeneration is unguided, sprouting fibres establish new connections 'blindly', changing the branching structure of nerves in the hand[6-8]. Digital nerves may reroute or exchange between digits. This would alter the typical orderly arrangement of digit maps in S1, and thus the pattern of interdigit response separability. The pattern would become atypical, as we have found.

A peripheral rewiring account is consistent with other evidence. Topographical changes in nerve transection and repair have been documented throughout the input pathway—in the hand, spinal cord, cuneate nucleus, and S1—and at each level, the changes exhibit common characteristics: they are highly idiosyncratic and restricted to the territory of the involved nerve[9-13]. When the major forelimb nerves are purposefully swapped, the maps in S1 reflect this[21]. In nerve crush injuries, normal S1 topography is restored, presumably because the structural elements of peripheral nerve remain intact, allowing nerve regeneration to proceed with guidance[42].

Deafferentation alone is unlikely to explain our findings. In hand amputation[31,43] as well as spinal cord injury (tetraplegia)[44], the pattern of interdigit response separability, measured using representational distances typicality, is within the normative range of healthy controls. This directly contrasts with our results.

Additionally, in tetraplegia, typicality decreases with increasing time since injury[44]. Exploratory tests with our data reveal no significant correlations between typicality and time-since-repair (Supplementary Fig. S6).

Our findings also reveal less pronounced changes in patients with isolated ulnar nerve repairs. This too may be explained by changes in peripheral topography. The ulnar nerve innervates fewer digits, restricting the possible spatial spread of rewiring.

Of course, without direct measures of reinnervation errors a peripheral rewiring account remains tentative. As a compromise, we measured locognosia error and assumed that this would constitute a valid proxy for reinnervation errors[24,25,35]. Future research would benefit from more direct measures (for e.g., using microneurography[25,45]).

We also observe changes in typicality within the hemisphere ipsilateral to nerve repairs, driven by responses from the patient's healthy hand. These findings cannot be explained by direct effects of peripheral rewiring, and were not predicted. We offer two interpretations. First, these effects may reflect a form of plasticity transfer between hemispheres[46-49]. Contrary to classic conceptualizations, increasing evidence now suggests that the functional role of S1 is inherently bilateral, processing and integrating information from both hands[50]. This tight coupling between hands may facilitate an exchange of plasticity, driving our results.

A second interpretation is that altered cortical maps reflect compensatory changes in the way patients use their hands in everyday life. The healthy hand, in particular, may assume different roles, and bimanual behaviour is likely to fundamentally change. Perhaps atypical patterns of interdigit response separability reflect these changes. Notably, 10 (of 21) patients in our study injured their dominant hand.

Clinical significance

Contemporary models of functional recovery in nerve repair place a strong emphasis on the brain and its capacity for change[4,13,49,51-56]. The functional maps of the hand in S1 are presumed to reorganise in accordance with animal models, and functional recovery is conceptualised as a process of relearning in the brain. Recovery depends

on reversing the changes in S1 or facilitating different parts of the brain to adapt accordingly.

By providing the first compelling evidence for altered digit maps after nerve repair in humans, our study validates a core assumption of contemporary therapeutic models—nerve repair indeed alters the cortical maps of the hand. Until now, this had only been shown in animals. Nonetheless, the functional significance of these findings remains unclear. According to our results, altered digit maps do not correlate with impairments in touch localisation or with broader measures of functional impairment as captured by Sensory Rosen scores.

We are surprised by these results. Impaired locognosia in patients and reorganised S1 topography in animals exhibit common characteristics, such as restricted occurrence within nerve-injured zones and high individual variability[10]. Further, reinnervation errors are proposed to explain both impaired locognosia[24,25] and reorganised S1 topography[21]. We expected patients with more pronounced localisation impairments to exhibit more pronounced differences in S1 organisation. We did not find this.

One potential concern is that our methods measure locognosia error within digits but S1 organisation between digits. Misreferrals were too infrequent to permit appropriate quantitative analyses. Future work could address this using adaptive psychophysical methods designed to elicit frequent misreferrals[57,58]. Alternatively, intradigit organisation could be mapped using ultra-high field fMRI[59,60].

Conclusions

We show that hand-nerve repair significantly alters the functional organisation of S1, yet the clinical significance of these changes remains unclear. Given the inherent heterogeneity of peripheral nerve injuries and the complexity of factors influencing patient recovery[54], future research would benefit from longitudinal measures and more advanced modelling methods to investigate whether and how brain changes relate to patient outcomes. This question remains of great fundamental and clinical significance.

Data availability

Summary data are available at github.com/weberetal/fMRI_PNR

Acknowledgements

David McKiernan provided technical support, and Rebecca Henderson coordinated participant visits. We also thank all participants for their involvement.

Funding

K.F.V. was supported by a grant from the Wellcome Trust (215186/Z/19/Z).

Competing interests

The authors report no competing interests.

References

1. Murphy RNA, de Schoulepnikoff C, Chen JHC, et al. The incidence and management of peripheral nerve injury in England (2005-2020). *J Plast Reconstr Aesthet Surg*. May 2023;80:75-85. doi:10.1016/j.bjps.2023.02.017
2. Rosberg HE, Carlsson KS, Hojgard S, Lindgren B, Lundborg G, Dahlin LB. Injury to the human median and ulnar nerves in the forearm--analysis of costs for treatment and rehabilitation of 69 patients in southern Sweden. *J Hand Surg Br*. Feb 2005;30(1):35-9. doi:10.1016/j.jhsb.2004.09.003
3. Rosen B, Lundborg G. The long term recovery curve in adults after median or ulnar nerve repair: a reference interval. *J Hand Surg Br*. Jun 2001;26(3):196-200. doi:10.1054/jhsb.2001.0567
4. Lundborg G, Rosen B. Hand function after nerve repair. *Acta Physiol (Oxf)*. Feb 2007;189(2):207-17. doi:10.1111/j.1748-1716.2006.01653.x
5. Brushart TM. *Nerve Repair*. Oxford University Press; 2011.
6. Witzel C, Rohde C, Brushart TM. Pathway sampling by regenerating peripheral axons. *J Comp Neurol*. May 9 2005;485(3):183-90. doi:10.1002/cne.20436
7. Lundborg G, Dahlin L, Danielsen N, Zhao Q. Trophism, tropism, and specificity in nerve regeneration. *J Reconstr Microsurg*. Sep 1994;10(5):345-54. doi:10.1055/s-2007-1006604
8. Brushart TM. Preferential motor reinnervation: a sequential double-labeling study. *Restor Neurol Neurosci*. Jan 1 1990;1(3):281-7. doi:10.3233/RNN-1990-13416
9. Paul RL, Goodman H, Merzenich M. Alterations in mechanoreceptor input to Brodmann's areas 1 and 3 of the postcentral hand area of Macaca mulatta after nerve section and regeneration. *Brain Res*. Apr 14 1972;39(1):1-19.
10. Wall JT, Kaas JH, Sur M, Nelson RJ, Felleman DJ, Merzenich MM. Functional reorganization in somatosensory cortical areas 3b and 1 of adult monkeys after median nerve repair: possible relationships to sensory recovery in humans. *J Neurosci*. Jan 1986;6(1):218-33.
11. Merzenich MM, Jenkins WM. Reorganization of cortical representations of the hand following alterations of skin inputs induced by nerve injury, skin island transfers, and experience. *J Hand Ther*. Apr-Jun 1993;6(2):89-104.
12. Florence SL, Garraghty PE, Wall JT, Kaas JH. Sensory afferent projections and area 3b somatotopy following median nerve cut and repair in macaque monkeys. *Cereb Cortex*. Jul-Aug 1994;4(4):391-407.
13. Florence SL, Boydston LA, Hackett TA, Lachoff HT, Strata F, Niblock MM. Sensory enrichment after peripheral nerve injury restores cortical, not thalamic, receptive field organization. *Eur J Neurosci*. May 2001;13(9):1755-66. doi:10.1046/j.0953-816x.2001.01555.x
14. Pons TP, Wall JT, Garraghty PE, Cusick CG, Kaas JH. Consistent features of the representation of the hand in area 3b of macaque monkeys. *Somatosens Res*. 1987;4(4):309-31. doi:10.3109/07367228709144612

15. Delhaye BP, Long KH, Bensmaia SJ. Neural Basis of Touch and Proprioception in Primate Cortex. *Compr Physiol*. Sep 14 2018;8(4):1575-1602. doi:10.1002/cphy.c170033

16. Qi HX, Kaas JH. Myelin stains reveal an anatomical framework for the representation of the digits in somatosensory area 3b of macaque monkeys. *J Comp Neurol*. Sep 13 2004;477(2):172-87. doi:10.1002/cne.20247

17. DiCarlo JJ, Johnson KO, Hsiao SS. Structure of receptive fields in area 3b of primary somatosensory cortex in the alert monkey. *J Neurosci*. Apr 1 1998;18(7):2626-45. doi:10.1523/JNEUROSCI.18-07-02626.1998

18. Merzenich MM, Kaas JH, Wall JT, Sur M, Nelson RJ, Felleman DJ. Progression of change following median nerve section in the cortical representation of the hand in areas 3b and 1 in adult owl and squirrel monkeys. *Neuroscience*. Nov 1983;10(3):639-65.

19. Merzenich MM, Kaas JH, Wall J, Nelson RJ, Sur M, Felleman D. Topographic reorganization of somatosensory cortical areas 3b and 1 in adult monkeys following restricted deafferentation. *Neuroscience*. Jan 1983;8(1):33-55.

20. Merzenich MM, Nelson RJ, Stryker MP, Cynader MS, Schoppmann A, Zook JM. Somatosensory cortical map changes following digit amputation in adult monkeys. *J Comp Neurol*. Apr 20 1984;224(4):591-605. doi:10.1002/cne.902240408

21. Wall JT, Kaas JH. Long-term cortical consequences of reinnervation errors after nerve regeneration in monkeys. *Brain Res*. May 7 1986;372(2):400-4.

22. Ejaz N, Hamada M, Diedrichsen J. Hand use predicts the structure of representations in sensorimotor cortex. *Nat Neurosci*. Jul 2015;18(7):1034-40. doi:10.1038/nn.4038

23. Sadnicka A, Wiestler T, Butler K, et al. Intact finger representation within primary sensorimotor cortex of musician's dystonia. *Brain*. Apr 19 2023;146(4):1511-1522. doi:10.1093/brain/awac356

24. Hawkins GL. Faulty sensory localization in nerve regeneration; an index of functional recovery following suture. *J Neurosurg*. Jan 1948;5(1):11-8. doi:10.3171/jns.1948.5.1.0011

25. Hallin RG, Wiesenfeld Z, Lindblom U. Neurophysiological studies on patients with sutured median nerves: faulty sensory localization after nerve regeneration and its physiological correlates. *Exp Neurol*. Jul 1981;73(1):90-106. doi:0014-4886(81)90047-9 [pii]

26. Smith SM, Jenkinson M, Woolrich MW, et al. Advances in functional and structural MR image analysis and implementation as FSL. *Neuroimage*. 2004;23 Suppl 1:S208-19. doi:10.1016/j.neuroimage.2004.07.051

27. Greve DN, Fischl B. Accurate and robust brain image alignment using boundary-based registration. Evaluation Study. *NeuroImage*. Oct 15 2009;48(1):63-72. doi:10.1016/j.neuroimage.2009.06.060

28. Yousry TA, Schmid UD, Alkadhi H, et al. Localization of the motor hand area to a knob on the precentral gyrus. A new landmark. *Brain*. Jan 1997;120 (Pt 1):141-57.

29. Dice LR. Measures of the amount of ecological association between species. *Ecology*. 1945;26:297–302. doi:10.2307/1932409

30. Kriegeskorte N, Diedrichsen J. Peeling the Onion of Brain Representations. *Annu Rev Neurosci*. Jul 8 2019;42:407-432. doi:10.1146/annurev-neuro-080317-061906

31. Kikkert S, Kolasinski J, Jbabdi S, et al. Revealing the neural fingerprints of a missing hand. *Elife*. Aug 23 2016;5doi:10.7554/eLife.15292

32. Sanders ZB, Dempsey-Jones H, Wesselink DB, et al. Similar somatotopy for active and passive digit representation in primary somatosensory cortex. *Hum Brain Mapp*. Jun 15 2023;44(9):3568-3585. doi:10.1002/hbm.26298

33. Nili H, Wingfield C, Walther A, Su L, Marslen-Wilson W, Kriegeskorte N. A toolbox for representational similarity analysis. *PLoS Comput Biol*. Apr 2014;10(4):e1003553. doi:10.1371/journal.pcbi.1003553

34. Wesselink D, Maimon-Mor R. rsatoolbox. 20fbe05. Github. https://github.com/ronimaimon/rsatoolbox

35. Weber M, Marshall A, Timircan R, et al. Touch localization after nerve repair in the hand: insights from a new measurement tool. *J Neurophysiol*. Nov 1 2023;130(5):1126-1141. doi:10.1152/jn.00271.2023

36. Rosen B, Lundborg G. A model instrument for the documentation of outcome after nerve repair. *J Hand Surg Am*. May 2000;25(3):535-43. doi:10.1053/jhsu.2000.6458

37. Hakir. National Assessment Manual: For assessment of hand function after nerve repair. 2018. https://hakir.se/about-hakir/

38. Puigdellivol-Sanchez A, Prats-Galino A, Molander C. On regenerative and collateral sprouting to hind limb digits after sciatic nerve injury in the rat. *Restor Neurol Neurosci*. 2005;23(2):97-107.

39. Koerber HR, Mirnics K, Brown PB, Mendell LM. Central sprouting and functional plasticity of regenerated primary afferents. *J Neurosci*. Jun 1994;14(6):3655-71. doi:10.1523/JNEUROSCI.14-06-03655.1994

40. Koerber HR, Seymour AW, Mendell LM. Mismatches between peripheral receptor type and central projections after peripheral nerve regeneration. *Neurosci Lett*. Apr 24 1989;99(1-2):67-72. doi:10.1016/0304-3940(89)90266-8

41. Logothetis NK, Wandell BA. Interpreting the BOLD signal. *Annu Rev Physiol*. 2004;66:735-69.

42. Wall JT, Felleman DJ, Kaas JH. Recovery of normal topography in the somatosensory cortex of monkeys after nerve crush and regeneration. *Science*. Aug 19 1983;221(4612):771-3.

43. Wesselink DB, van den Heiligenberg FM, Ejaz N, et al. Obtaining and maintaining cortical hand representation as evidenced from acquired and congenital handlessness. *Elife*. Feb 5 2019;8doi:10.7554/eLife.37227

44. Kikkert S, Pfyffer D, Verling M, Freund P, Wenderoth N. Finger somatotopy is preserved after tetraplegia but deteriorates over time. *Elife*. Oct 19 2021;10doi:10.7554/eLife.67713

45. Moore CEG. Evidence of preferential sensory reinnervation in man: a study of nine patients. *J Hand Surg Eur Vol*. Sep 2021;46(7):781-783. doi:10.1177/1753193421998971

46. Valyear KF, Philip BA, Cirstea CM, et al. Interhemispheric transfer of post-amputation cortical plasticity within the human somatosensory cortex. *Neuroimage*. Feb 1 2020;206:116291. doi:10.1016/j.neuroimage.2019.116291

47. Pelled G, Chuang KH, Dodd SJ, Koretsky AP. Functional MRI detection of bilateral cortical reorganization in the rodent brain following peripheral nerve deafferentation. *Neuroimage*. Aug 1 2007;37(1):262-73. doi:10.1016/j.neuroimage.2007.03.069

48. Li N, Downey JE, Bar-Shir A, et al. Optogenetic-guided cortical plasticity after nerve injury. *Proc Natl Acad Sci U S A*. May 24 2011;108(21):8838-43. doi:10.1073/pnas.1100815108

49. Sparling T, Iyer L, Pasquina P, Petrus E. Cortical Reorganization after Limb Loss: Bridging the Gap between Basic Science and Clinical Recovery. *J Neurosci*. Jan 3 2024;44(1)doi:10.1523/JNEUROSCI.1051-23.2023

50. Tame L, Braun C, Holmes NP, Farne A, Pavani F. Bilateral representations of touch in the primary somatosensory cortex. *Cogn Neuropsychol*. Feb-Mar 2016;33(1-2):48-66. doi:10.1080/02643294.2016.1159547

51. Mohanty CB, Bhat D, Devi BI. Role of Central Plasticity in the Outcome of Peripheral Nerve Regeneration. *Neurosurgery*. Sep 2015;77(3):418-23. doi:10.1227/NEU.0000000000000851

52. Li C, Liu SY, Pi W, Zhang PX. Cortical plasticity and nerve regeneration after peripheral nerve injury. *Neural Regen Res*. Aug 2021;16(8):1518-1523. doi:10.4103/1673-5374.303008

53. Anastakis DJ, Chen R, Davis KD, Mikulis D. Cortical plasticity following upper extremity injury and reconstruction. *Clin Plast Surg*. Oct 2005;32(4):617-34, viii. doi:10.1016/j.cps.2005.05.008

54. Lundborg G. *Nerve injury and repair: regeneration, reconstruction, and cortical remodeling*. 2nd ed. Elsevier/Churchill Livingstone; 2004.

55. Rosen B, Vikstrom P, Turner S, et al. Enhanced early sensory outcome after nerve repair as a result of immediate post-operative re-learning: a randomized controlled trial. *J Hand Surg Eur Vol*. Jul 2015;40(6):598-606. doi:10.1177/1753193414553163

56. Lundborg G. Richard P. Bunge memorial lecture. Nerve injury and repair--a challenge to the plastic brain. *J Peripher Nerv Syst*. Dec 2003;8(4):209-26. doi:10.1111/j.1085-9489.2003.03027.x

57. Schweizer R, Maier M, Braun C, Birbaumer N. Distribution of mislocalizations of tactile stimuli on the fingers of the human hand. *Somatosens Mot Res*. 2000;17(4):309-16. doi:10.1080/08990220020002006

58. Braun C, Ladda J, Burkhardt M, Wiech K, Preissl H, Roberts LE. Objective measurement of tactile mislocalization. *IEEE Trans Biomed Eng*. Apr 2005;52(4):728-35. doi:10.1109/TBME.2005.845147

59. Sanchez-Panchuelo RM, Besle J, Mougin O, et al. Regional structural differences across functionally parcellated Brodmann areas of human primary somatosensory cortex. *Neuroimage*. Jun 2014;93 Pt 2:221-30. doi:10.1016/j.neuroimage.2013.03.044

60. Asghar M, Sanchez-Panchuelo R, Schluppeck D, Francis S. Two-Dimensional Population Receptive Field Mapping of Human Primary Somatosensory Cortex. *Brain Topogr*. Nov 2023;36(6):816-834. doi:10.1007/s10548-023-01000-8

Online Supplementary Materials

Cutting a nerve of the hand alters the organisation of digit maps in primary somatosensory cortex

Martin Weber[1], Andrew Marshall[2], Ronan Timircan[1], Francis McGlone[3], Raffaele Tucciarelli[4], Obi Onyekwelu[5], Louise Booth[6], Edwin Jesudason[6], Vivien Lees[7,8], and Kenneth F. Valyear[1,9]

1. School of Psychology and Sport Science, Bangor University, Bangor, United Kingdom
2. Department of Musculoskeletal Biology, Institute of Life Course and Medical Sciences, University of Liverpool, Liverpool, United Kingdom
3. School of Life Sciences, Faculty of Science & Engineering, Manchester Metropolitan University, United Kingdom
4. School of Psychological Sciences, Birkbeck, University of London, London, United Kingdom
5. Department of Plastic Surgery, Portsmouth Hospitals University NHS Trust, Cosham, United Kingdom
6. Department of Orthopaedics and Trauma, Betsi Cadwaladr University Health Board, Bangor, United Kingdom
7. Department of Plastic Surgery, University of Manchester, Manchester, United Kingdom
8. Manchester University Foundation Hospitals Trust, Manchester, United Kingdom
9. Bangor Imaging Unit, Bangor University, Bangor, United Kingdom

Supplementary Methods

Patients

Supplementary Table S1 provides patient demographics, standardised clinical assessment scores, and locognosia performance for their repaired hand.

Supplementary Table S1 Patient demographics, standardised clinical assessments, and locognosia performance

Subject ID	Demographics					Standardised Clinical Assessments				Locognosia[f]	
	Sex	WS[a]	MSR	Side	Nerve	DASH[b]	McGill[c]	Rosen		Error	Mis.
								Sensory[d]	Pain[e]		
21	F	28	19	L	M	29	15	0.15	0.17	11.3	0.40
22	M	30	10	L	U	21	3	0.23	0.33	16.5	0.02
25	M	30	60	R	U	66	14	0.51	0	10.3	0.04
26	F	30	37	R	M+U	53	13	0.13	--	14.3	0.13
27	F	-8	62	R	U	4	1	0.86	0.67	4.1	0.13
30	F	30	26	L	U	10	0	0.58	0.67	4.3	0.00
31	M	15	75	R	U	33	20	0.86	0.67	6.3	0.00
32	M	30	82	R	M+U	22	14	0.28	0.5	19.5	0.27
33	F	29	11	L	M	18	1	0.26	0.5	10.6	0.06
34	F	30	8	L	M+U	28	17	0.00	0	22.6	0.50
35	M	30	28	L	M+U	26	15	0.18	0.5	16.2	0.07
36	M	30	139	R	U	3	29	0.0	0.67	--	--
38	M	30	18	R	M+U	15	4	0.14	0.5	16.6	0.07
39	M	30	30	L	M[g]	21	36	0.60	1.0	8.4	0.01
40	M	22	31	R	M[g]	3	1	0.94	0.83	4.8	0.01
42	F	27	45	R	U	8	2	0.23	0.67	5.8	0.02
46	M	30	49	L	M[g]	0	0	0.91	1.0	8.3	0.00
47	M	-29	89	L	U	27	42	0.18	0.33	--	--
57	M	-30	130	R	U	9	3	0.25	0.67	12.0	0.14
61	M	3	40	L	U	23	5	0.29	0.67	9.5	0.03
63	M	30	7	R	M	55	16	0.34	0.33	32.8	0.18

Sex: F = female, M = male; WS = Waterloo score; MSR = months since repair; Side: L = left, R = right; Nerve: M = median, U = ulnar, M+U = combined median and ulnar repairs; Mis. = Misreferrals. -- indicates missing values.

[a] Modified Waterloo Handedness Inventory[1] is a questionnaire used to evaluate hand preference. Scores range from -30 to 30, where negative values indicate left-hand preference, and positive values indicate right-hand preference.

[b] The Disabilities of the Arm, Shoulder and Hand (DASH)[2] is a patient-reported outcome questionnaire where scores indicate the level of difficulty experienced using the upper limb to perform activities of daily living. A score of 0 indicates no difficulty; a score of 100 indicates maximal difficulty. This is a general test of upper limb function, not specific to nerve injury.

[c] The short-form McGill[3] questionnaire is a patient-reported outcome where scores reflect the severity of pain experienced. A score of 0 indicates no pain; a score of 45 indicates maximal pain.

[d] The sensory Rosen[4] test produces a single composite score, with subtests measuring touch detection thresholds using Semmes-Weinstein monofilaments, two-point discrimination, shape-texture-identification[5], and the Sollerman[6] hand function subtests 4, 8, and 10. Higher scores indicate better function, with a score of 1 indicating no impairment. A score of 0 indicates maximal impairment (i.e., no sub-tests were completed successfully).

[e] The Pain domain of the Rosen test is a patient-reported outcome questionnaire that evaluates pain and discomfort due to nerve injury. Higher scores indicate less pain/discomfort, with a score of 1 indicating no/minor pain/discomfort. A score of 0 indicates maximal pain/discomfort (i.e., "hinders function").

[f] Locognosia was evaluated using the Digital Photograph Method[7]. Error is the absolute error of localisation in mm, excluding misreferrals. Misreferrals are errors made between digits or from a digit to the palm, expressed in the table as proportions (i.e., the total number of misreferrals divided by the total number of stimulation trials). Notably, data were previously reported in Weber et al.[7] using different subject IDs, labelled as "P", but the participant order presented here remains unchanged: ID21 = P1, ID22 = P2, and so on, up to ID61 = P18. ID63 was tested more recently.

[g] Patients with incomplete nerve transection injuries.

MRI

Supplementary Fig. S1 gives a schematic of the experimental design for a single fMRI run, and picture of the setup in the scanner. The participant is positioned with the piezoelectric stimulators in place over the fingertips of their right hand.

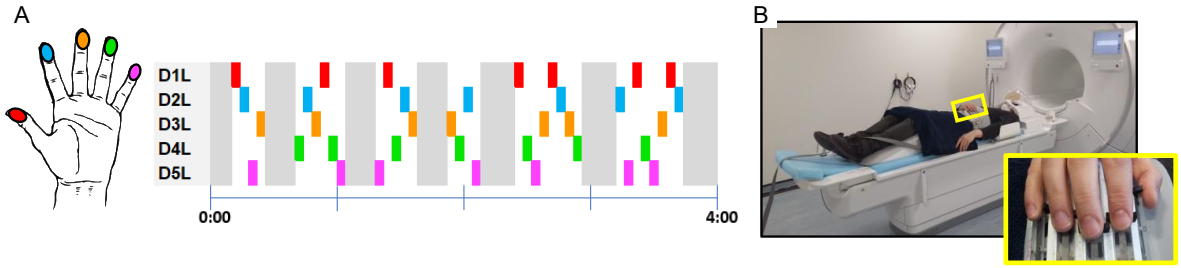

Figure S1. Functional MRI design and setup. A: An example of a single run. Each digit is stimulated seven times in the run, with periods of rest interspersed throughout. Each hand was tested separately. D1L = left thumb; D2L = left index finger; D3L = left middle finger; D4L = left ring finger; D5L = left little finger. **B:** An image of the participant setup in the scanner. The inset shows the piezoelectric stimulators.

Evaluating hypotheses

Statistical comparisons between patients and controls used unpaired t tests. This includes tests of S1-repaired versus S1-controls, where differences are predicted, and S1-healthy versus S1-controls, where differences are not predicted. If the variances between groups were unbalanced, a Welch's correction was applied. Direct comparisons within patients, i.e., S1-repaired versus S1-healthy, used paired t tests. For both between and within groups tests, if the residuals were not normally distributed, as measured using Shapiro–Wilk, nonparametric tests were applied (Mann–Whitney or Wilcoxon matched-pairs signed-rank tests, accordingly).

Repair-zone-specific analyses

To test whether brain changes are specific to the cortical zone of the repaired nerves, we repeated tests of H_1 using only those dice-coefficients/representational-distances computed based on comparisons between maps within the nerve repair zone. For patients with isolated median nerve repairs, this includes D1-D2, D1-D3, D1-D4, D2-D3, D2-D4 and D3-D4; for isolated ulnar nerve repairs, this includes D4-D5; for patients with combined median and ulnar nerve injuries, all pairwise digit-map comparisons comprise the repair zone and are included (see Fig. 3C-ii and Fig. 4C-ii of the main text for illustration). Mean dice coefficients and representational-distances are computed for S1-repaired and S1-healthy, accordingly.

We then needed to organise our data from healthy controls so that fair comparisons between patients and controls could be made. Otherwise, group comparisons would involve

group-mean-estimates of dice coefficients and representational distances from different combinations of pairwise digit maps. As such, the controls' data were formulated to 'match' the proportions of patients with median/ulnar/both nerve injuries. Specifically, six patients had isolated median nerve injuries (~29% of the group); thus 9 controls were treated as median-nerve-injured (30% of the group). This meant that the data from these 9 controls comprised estimates of interdigit separability from D1-D2, D1-D3, D1-D4, D2-D3, D2-D4 and D3-D4 comparisons. In the same fashion, 10 patients had isolated ulnar nerve injuries (~ 48%), and so, 14 controls were assigned to match these patients (~ 47% of the control group). Their data comprised D4-D5 comparisons, matching the ulnar patients. The remaining proportion of controls (7 controls in total) were matched against the patients with both median and ulnar nerve injuries. Their data were taken from all pairwise digit comparisons. The assignment of controls to patient subgroups was otherwise random.

Locognosia

The digital photograph method was used to evaluate touch localisation; see Weber et al.[7] for complete methodological details and procedures.

Supplementary Fig. S2A shows a picture of the setup and apparatus. The participant places their hand in the apparatus with the palm facing up, and the experimenter stimulates UV-marked targets on the surface using a 6.1 Semmes-Weinstein monofilament. Fig. S2B shows the configuration of targets. This is an example from one participant, with targets visible under UV lighting in the left picture and invisible under normal lighting on the right. The absolute error is calculated as the Euclidian distance between target-response pairs in millimetres, excluding misreferrals—responses made to an incorrect digit, or to the palm of the hand (Fig. S2C).

To evaluate impairment, targets on the patient's repaired hand are defined as within or outside the territory of the repaired nerve(s). Fig. S2D shows the targets within the repaired nerve zone for isolated median and ulnar nerve patients, respectively. For median nerve repairs, these targets comprise all locations on digits D1-to-D4 (14 targets). For ulnar nerve repairs, these targets comprise all locations on digits D4 and D5 (8 targets). For patients with both median and ulnar nerve repairs, all targets are defined as within the nerve repair zone.

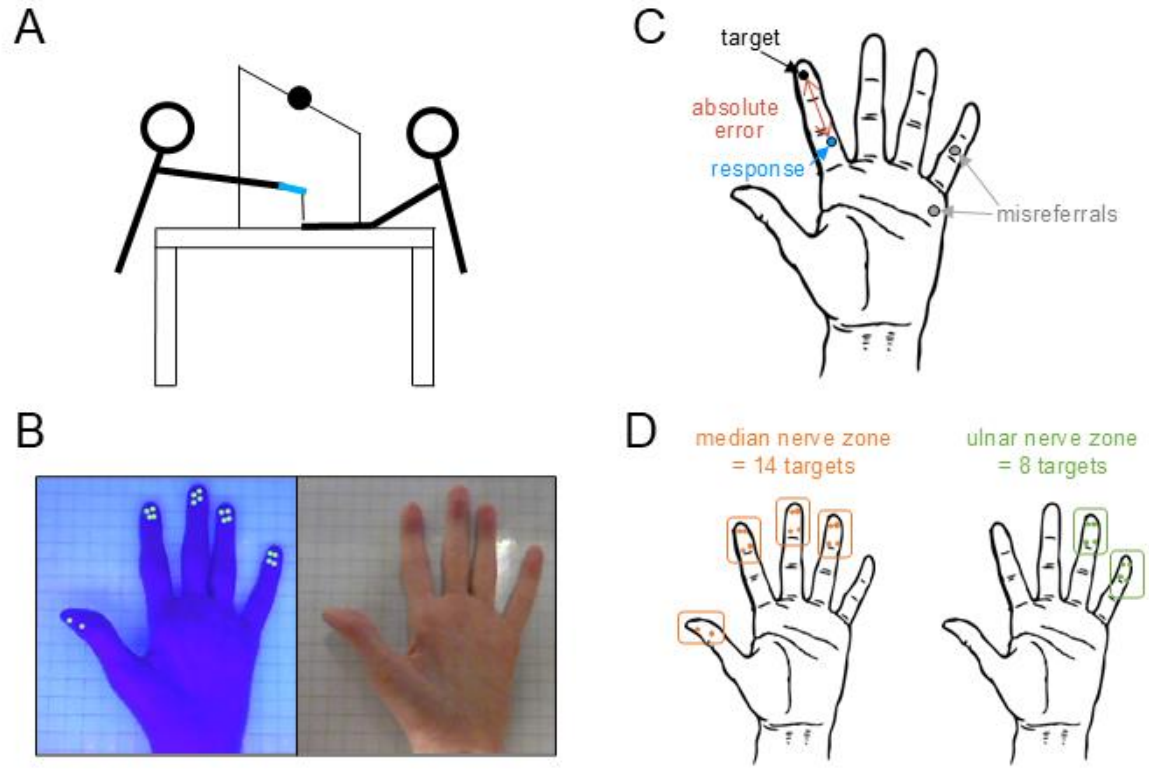

Figure S2. Locognosia testing: Digital photograph method. A: Schematic of the experimenter (left) and participant (right) in position during testing. The participant's hand is through a 'blinder box' to obscure their vision of the hand, and the experimenter applies stimulation using a monofilament. **B**: UV-light image (left) used by the experimenter to register targets and a normal light image (right) on which the participant registers their responses. **C**: The target is the location where the experimenter applies the touch stimulus. Response is where the participant indicates they felt they were touched. The absolute localization error is computed as the Euclidian distance between target and response. Responses made to another digit or to the palm are defined as misreferrals. **D**: Targets defined as within the repair zone for median (left, orange) and ulnar (right, green) nerve repairs. Part of this figure has been modified from Weber et al.[7], licensed under CC-BY.

Two patients were unable to open their hand sufficiently to complete this test. Their fingers curled inward towards the palm, due to associated tendon injuries. Thus, as reported in the main text, 19 of 21 patients completed locognosia testing.

Supplementary Results

Averaged controls' data between hands

Data from healthy controls were defined separately for each hand, extracted from the contralateral S1 ROI of each hemisphere, and then averaged between hands. In principle, this approach could confound results of comparisons against patients, where responses to each hand are kept separate. If healthy controls exhibit differences in responses between hands,

taking the average of both hands to compare against patient's data could introduce artificial differences, or obscure true differences.

One test revealed differences between dominant and non-dominant hands in healthy controls. This was the test evaluating mean representational distances, collapsed across all pairwise interdigit map comparisons. Here, the data reveal greater representational distances for the non-dominant hand ($t(29) = 2.3$, $p = 0.03$). This indicates that according to multivariate representational distances, interdigit responses in S1 are more separable for the non-dominant versus the dominant hand.

This result necessitates additional tests to validate results and conclusions made in the main text. Specifically, as reported, mean representational distances do not differ between patients and controls (See Fig. 4 and corresponding results in the main text). Are these results confounded by the fact that control participants show differences between dominant and non-dominant hands, while comparisons against patients are made after averaging the controls data between hands? In other words, could there be a true difference between patients and controls that is being obscured by averaging the controls data between hands?

Results of the following tests rule out this possibility. First, we generated a 'simulated S1-repaired' group from our controls data based on the proportion of patients who injured their dominant/non-dominant hands. Specifically, there are 10 patients with injuries to their dominant hand (~48% of the group). Thus, 14 controls were treated as having an injury to their dominant hand (~48% of the group). This meant that the data from these 14 controls comprised their dominant hand responses. The remaining controls data in the 'simulated S1-repaired' dataset comprised their non-dominant hand responses. This creates a mixture of dominant and non-dominant hand controls data that 'matches' the proportions comprising the patient's data. The assignment of controls to was otherwise random. Comparisons then revealed still no differences between patients and controls: S1-repaired (patients) versus 'simulated S1-repaired' (controls): Mann-Whitney $U = 285$, $p = 0.58$.

Second, even in the extreme case of comparing healthy controls data comprised entirely of results from their non-dominant hand versus S1-repaired (patients), we do not find statistical differences: Mann-Whitney $U = 246$, $p = 0.19$. In other words, there is no combination of controls data that would lead to different conclusions regarding comparisons against patients than those provided in the main text, based on controls data being averaged between hands.

No other variables showed significant inter-hand differences in healthy controls: dice coefficients: $t(29) = 1.7$, $p = 0.10$; dice typicality: $t(29) = 1.6$, $p = 0.13$; representational distances typicality: $t(29) = 0.97$, $p = 0.34$.

Do changes in S1 relate to functional impairments?

Misreferrals

Misreferrals are errors of touch localisation occurring between digits or from a digit to the palm. Given that most patients show a relatively low frequency of misreferrals within the range observed in healthy controls (as defined previously, based on data from 33 healthy controls[7]), interpreting results from quantitative group-level analyses is challenging. Supplementary Fig. S3 shows these results, plotting misreferrals made for the repaired hand against the three fMRI measures that showed evidence of nerve-repair-related changes in S1: dice coefficients, dice typicality, and representational distances typicality. Misreferrals are expressed as proportions relative to the total number of trials (i.e., 90 trials).

No reliable correlations are found. While the test of misreferrals against representational distances typicality yields a significant (uncorrected) correlation ($r(17) = -0.50$, $p = 0.03$), this is driven by a single patient. With this patient (ID34) excluded, the correlation is non-significant ($r(16) = -0.10$, $p = 0.68$). Similarly, no significant correlations are observed for average dice coefficients ($r(17) = -0.15$, $p = 0.54$) or dice typicality ($r(17) = -0.34$, $p = 0.15$).

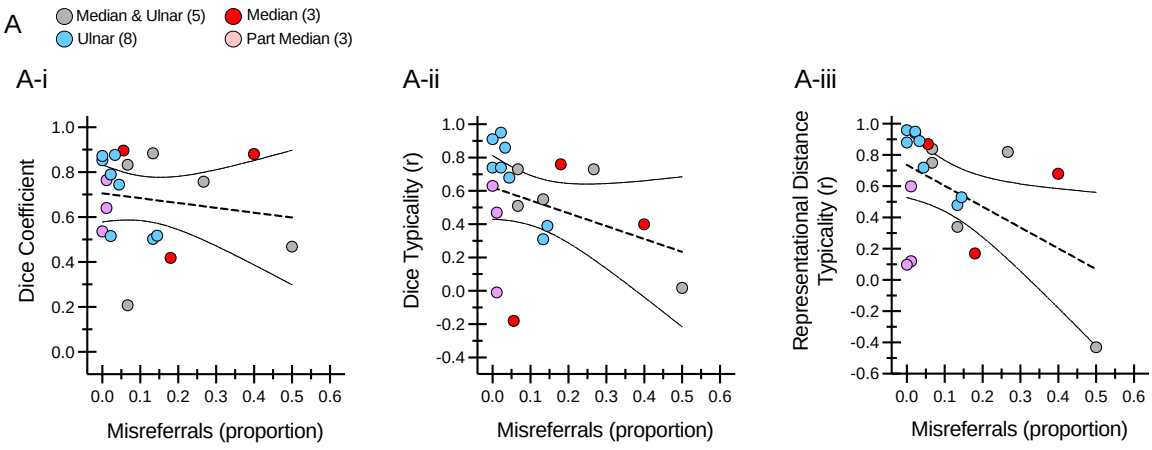

Figure S3. Misreferral frequency does not relate to S1 reorganisation. A: Group-level (n = 19) correlational tests of the frequency of misreferrals versus dice coefficients (A-i), dice typicality (A-ii), and representational distances typicality (A-iii). No reliable relationships are observed.

In the main text we present data from a single patient, ID21, who exhibits an usual pattern of misreferrals consistent with possible reinnervation errors ('rewiring') between digits. Only one other patient, ID32, demonstrates a comparable pattern. This patient injured both their median and ulnar nerves. Supplementary Fig. S4 provides their data, organised in the same way as Fig. 8 of the main text. Patient ID32 frequently misrefers touch of D5 to D4 and confuses D2 and D3; neither of which are typically observed in healthy controls[7].

As with ID21 and Fig. 8 of the main text, we offer these data for conceptual purposes only; no definitive conclusions can be made. Nonetheless, these single-case examples illustrate possible relationships between misreferrals, reinnervation errors, and altered digit maps. Making these descriptions available may be useful for future research.

As noted in main text (see Discussion), our fMRI measures evaluate brain organisation at the *interdigit* level—we measure the overall extent and pattern of separability of responses in S1 *between* digits—while our measures of touch localisation evaluate errors made *within* digits (absolute error of localisation). Although speculative, the observed absence of a relationship between fMRI findings and locognosia could be due to this relative mismatch in the levels of analyses. Future research may benefit from adaptive psychophysical methods that target patterns of misreferrals in ways that enable group-level quantitative statistical analyses[8,9].

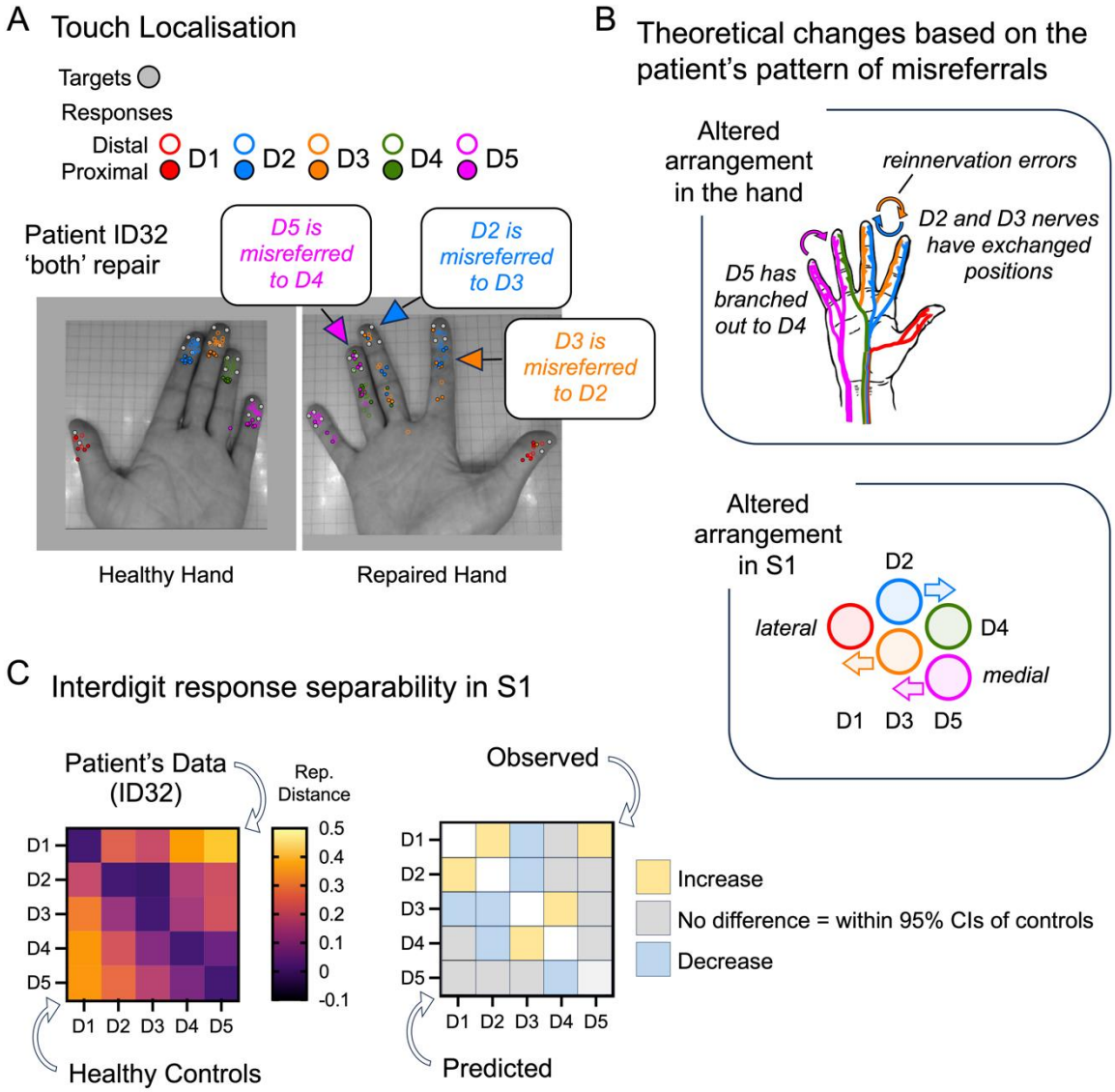

Figure S4. Frequent misreferrals between digits may reflect reinnervation errors: ID32. A: Locognosia results from patient ID32. Targets (grey circles) and responses (coloured circles) are overlaid on the photographs of the hand. The colours indicate which digits were touched (see inset key). Touch of D5 was frequently misreferred to D4, and D2 and D3 were often confused. **B:** Theoretical changes in the arrangement of nerves in the hand based on the patient's pattern of misreferrals. Reinnervation errors may have resulted in a nerve of D5 re-routed to D4, and nerves of D2 and D3 may have exchanged. This would predictably alter the arrangement of digit maps in S1. For example, D5 should 'move closer' to D4. **C:** Representational distances are shown in the heatmap, with patient ID32's data above the reference diagonal and the mean of healthy controls below (left). Predicted and observed differences between the patient's data and controls (right). The observed differences are above the reference diagonal and predicted differences are below. For each interdigit comparison, 'increased'/'decreased' observed results indicates that the patient's representational distances are above/below the 95% confidence intervals of healthy controls, respectively.

Sensory Rosen scores

Supplementary Fig. S5 shows the sensory Rosen scores plotted against the mean dice coefficients (Fig. S5A-i), dice typicality (Fig. S5A-ii), and representational distances typicality (Fig. S5A-iii). As reported in the main text, no significant correlations are observed.

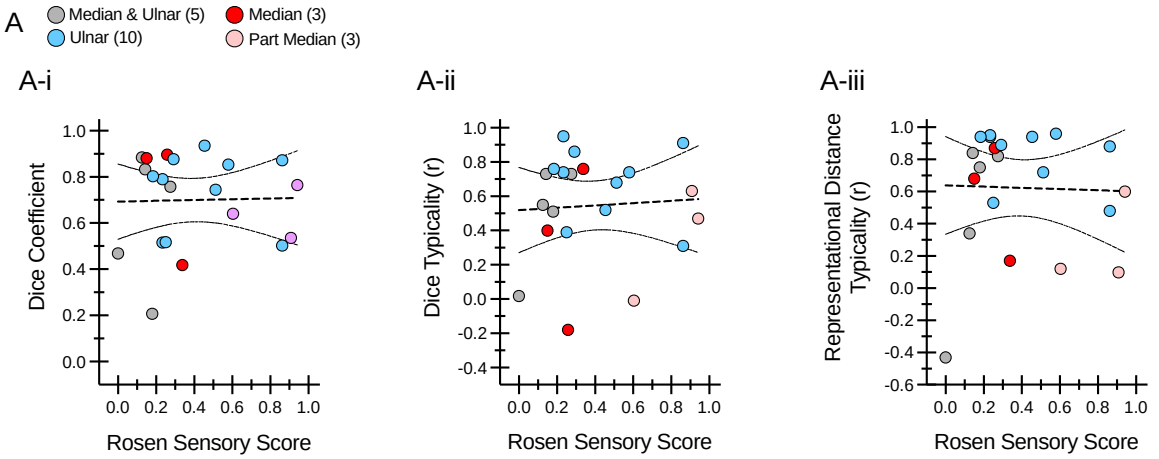

Figure S5. Sensory Rosen score does not relate to S1 reorganisation. A: Group-level (n = 21) correlational tests of sensory Rosen scores versus dice coefficients (A-i), dice typicality (A-ii), and representational distances typicality (A-iii). See main text for statistical results.

Time since nerve repair

We also assessed the relationship between time since repair and reorganizational changes in S1. The results reveal no reliable correlations between time-since-repair and dice coefficients (Fig. S6A-i; r(19) = 0.13, p = 0.58), dice typicality (Fig. S6A-ii; r(19) = 0.15, p = 0.51), or representational distances typicality (Fig. S6A-iii; r(19) = 0.28, p = 0.23).

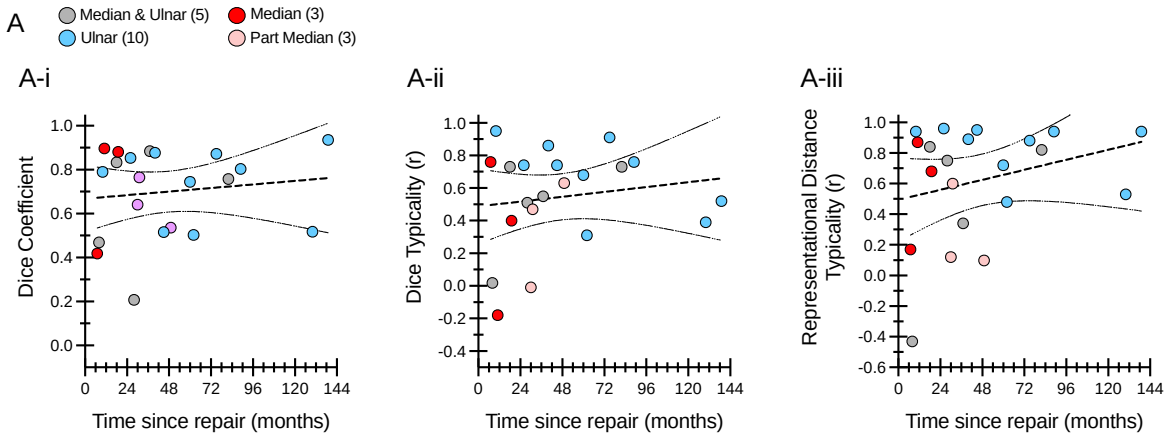

Figure S6. Time since nerve repair does not relate to S1 reorganisation. A: Group-level (n = 21) correlational tests of time since repair versus dice coefficients (A-i), dice typicality (A-ii), and representational distances typicality (A-iii).

References

1. Steenhuis RE, Bryden MP. Different dimensions of hand preference that relate to skilled and unskilled activities. *Cortex*. Jun 1989;25(2):289-304.
2. Hudak PL, Amadio PC, Bombardier C. Development of an upper extremity outcome measure: the DASH (disabilities of the arm, shoulder and hand) [corrected]. The Upper Extremity Collaborative Group (UECG). *Am J Ind Med*. Jun 1996;29(6):602-8. doi:10.1002/(SICI)1097-0274(199606)29:6<602::AID-AJIM4>3.0.CO;2-L
3. Melzack R. The short-form McGill Pain Questionnaire. *Pain*. Aug 1987;30(2):191-7.
4. Rosen B, Lundborg G. A model instrument for the documentation of outcome after nerve repair. *J Hand Surg Am*. May 2000;25(3):535-43. doi:10.1053/jhsu.2000.6458
5. Rosen B, Lundborg G. A new tactile gnosis instrument in sensibility testing. *J Hand Ther*. Oct-Dec 1998;11(4):251-7.
6. Sollerman C, Ejeskar A. Sollerman hand function test. A standardised method and its use in tetraplegic patients. *Scand J Plast Reconstr Surg Hand Surg*. Jun 1995;29(2):167-76.
7. Weber M, Marshall A, Timircan R, et al. Touch localization after nerve repair in the hand: insights from a new measurement tool. *J Neurophysiol*. Nov 1 2023;130(5):1126-1141. doi:10.1152/jn.00271.2023
8. Braun C, Ladda J, Burkhardt M, Wiech K, Preissl H, Roberts LE. Objective measurement of tactile mislocalization. *IEEE Trans Biomed Eng*. Apr 2005;52(4):728-35. doi:10.1109/TBME.2005.845147
9. Schweizer R, Maier M, Braun C, Birbaumer N. Distribution of mislocalizations of tactile stimuli on the fingers of the human hand. *Somatosens Mot Res*. 2000;17(4):309-16. doi:10.1080/08990220020002006